Multi-Phase Flow in a Thin Porous Material

Uwe Beuscher
W. L. Gore, Inc.
Industry Representative

Saziye Bayram, SUNY Buffalo
Philip Broadbridge, University of Delaware
Toby Driscoll, University of Delaware
David A. Edwards, University of Delaware
Joseph Fehribach, Worcester Polytechnic Institute
James Graham-Eagle, University of Massachusetts, Lowell
Ryan Haskett, Duke University
Alfa Heryudono, University of Delaware
Huaxiong Huang, York University
Dale Larson
Richard Moore, University of Delaware
Steve Pennell, University of Massachusetts, Lowell
Chris Raymond, New Jersey Institute of Technology
Bob Ronkese, University of Delaware
Lou Rossi, University of Delaware
Ravi Srinivasan, Worcester Polytechnic Institute
and others...

Twentieth Annual Workshop on Mathematical Problems in Industry
June 21–25, 2004
University of Delaware

Section 1: Introduction

Fuel cells offer the potential for delivering quiet, efficient power from stored hydrogen. While reverse electrolysis seems simple in principle, the reality is that fuel cells are complex, interrelated systems, involving coupled physical, chemical and electrical processes occurring in thin layers. To date, there has been little success decoupling the multitude of processes from one another, though progress in this area would open the door to analytic and computational treatment of the problem. A more complete description of some of the interdependent fields in shown in Figure 1.1.

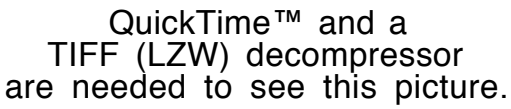

Figure 1.1. A schematic diagram of a more complete fuel cell model. The unknown fields include fluxes of hydrogen, oxygen, protons, electrons, water (both liquid and vapor), and heat. Even this model is simplified from the more complex reality which includes labyrinthine flow channels that deliver the gases to the GDL.

Since chemical reactions occur in very thin layers of distinct materials, experimental techniques for measuring certain physical parameters do not yet exist. Even if a large number of material parameters were known, it is not yet clear which parameters or combinations of parameters are significant from a design perspective. Thus, engineers and designers have encouraged the mathematical community to develop a deeper understanding the underlying processes in fuel cells and provide some physical insight and guidance

on their operation. Similarly, in the mathematics community, we find that fuel cells provide a rich source of problems for mathematicians with interests in modeling, analysis, and computation.

The 2004 MPI workshop problem from Gore is an attempt to gain physical intuition about some of the fundamental processes in a fuel cell. All three fuel cell problems focus on the diffusion layer in a simplified periodic geometry on the cathode side of the cell. The proposed problems were intended to be increasingly difficult though the second was found to be more regular than the first, thus offering some advantages. The original problem statement is included in Appendix B, but a summary diagram is shown in Figure 1.2.

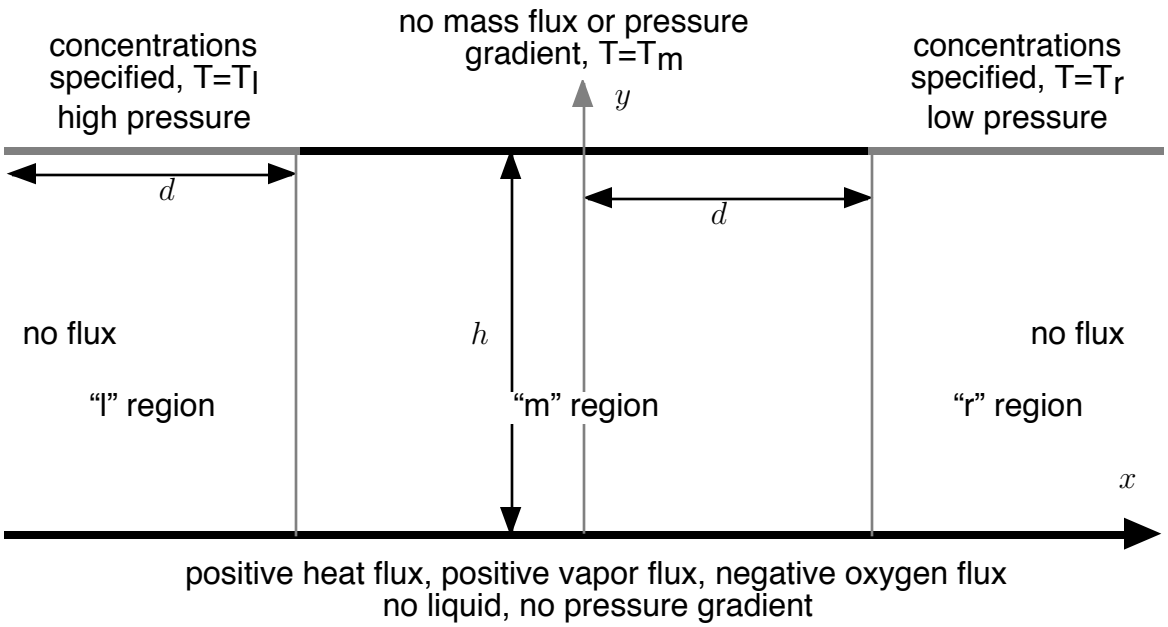

Figure 1.2. This simplified periodic geometry was the focus of our attention during the MPI workshop. The grey lines at the top of the diagram indicate the position of the channel through which the gases flow. We consider only the movement of gas, liquid water, vapor and heat through the rightmost GDM in Figure 1. Note also that the orientation of this diagram has been rotated 90° from Figure 1. (In particular, the cathode to the left of the GDM is now beneath it.)

On the bottom catalyst side, heat and water (in liquid and vapor phases) are added to the system, and gas is absorbed. On the upper channel side, heat and water are removed but gas is added. The problem is complicated by the fact that half the upper boundary is the solid cathode material and half is the open channel. Thus the fluid flow boundary conditions are mixed Neumann (no flux into the cathode) and Dirichlet (no liquid water in the channel).

To inspire our activities, we drew heavily from two sources, electrochemistry and hydrogeology. In the former body of literature, there has been some effort in the last decade to develop electrochemical models of fuel cells [1–3] or portions thereof [4–8]. In these areas, there has been significant activity in identifying the relevant physical processes

as well as simulating and analyzing these models in portions of fuel cell.

In the hydrogeological literature, detailed models exist for multiphase flow in unsaturated media with temperature dependence [9–12]. However, the moisture movement in these models depends strongly upon the moisture potential which includes material properties of the porous material. These properties, including the water content dependent permeability, are not known for the GDL, and may be exceedingly difficult to measure. While there are clear parallels for multiphase flow in the GDL and unsaturated soils, there are some important distinctions as well. The GDL is hydrophobic and soil is hydrophilic. This could have a significant effect on the movement of gases through slightly wetted material. Next, the pore size distributions are likely to be different. Finally, the GDL is a thin, paper-like weave of carbon fibers. Depending upon the manufacturing process, the weave may be disordered or woven into an orderly array. In either case, any GDL is likely to be an anisotropic medium.

This report is our week-long attempt to develop some mathematical insight into these problems. In section 2 we derive the governing equations for the most general case. In section 3 we specialize those equations to the case where no liquid water is present. Sections 4–6 address several cases of transport and flux conditions for this case. In sections 7 and 8 the issue of two-component gas diffusion is addressed. Section 9 addresses the transport of liquid water, while section 10 addresses the cases where all phases are present together.

Section 2: General Equations

We wish to model the transport of various species through the gas diffusion layer (GDL) diagrammed in Figure 1.2. The layer is made up of blocks, periodic in the long ($\tilde{x}$-)direction, that are $4d$ units long and h units high (the $\tilde{y}$-direction). The aspect ratio is small, so we define $\epsilon = h/d \ll 1$ as our perturbation parameter. The lower surface $\tilde{y} = 0$ abuts the cathode catalyst layer (CCL). The upper surface ($\tilde{y} = h$) is open to two channels, one on the left ($-2d \leq \tilde{x} \leq -d$) and one on the right ($d \leq \tilde{x} \leq 2d$). The region in the center ($|\tilde{x}| < d$) abuts a graphite cathode. All quantities are assumed to be in steady state. Each of the channels may be at a different pressure.

We wish to track the pressure $\tilde{P}$, temperature $\tilde{T}$, the oxygen concentration $\tilde{u}$, the water vapor concentration $\tilde{v}$ and liquid water volume fraction θ. It is important to note that in our work we assume that the vapor is in thermodynamic equilibrium owing to the fact that the GDL is very thin. In contrast, geophysical models do not make this assumption and capture the liquid and vapor water content in one variable. Since we are considering the volume fraction of the entire GDL, the correct range is $0 \leq \theta \leq \phi$, where ϕ is the porosity of the GDL. As the liquid water volume fraction increases, the water will begin to occlude the pores. Thus the diffusion coefficients, permeabilities, etc., will all be functions of θ.

The reader is directed to articles by Philip and Philip & DeVries [9,10] for a comprehensive treatment of liquid water and vapor transport in vadose (unsaturated) soils. The general form is given by Richard's equation,

$$\tilde{\mathbf{V}}_\theta = -\kappa_\theta(\theta)\nabla\Psi, \tag{2.1}$$

where $\tilde{\mathbf{V}}_\theta$ is the moisture velocity, κ_θ is the hydraulic conductivity of the GDL to liquid water, and Ψ is the moisture potential. In reality, the total potential would also have a gravitational component. We discard it from consideration because in the normal fuel cell operating regime, very little liquid water is present. Thus θ is small and Ψ gradients are large, so gravity is negligible over the thin GDL. The moisture potential must include all the distinctive material properties of the GDL such as wetting potential, tortuosity, etc.

The important feature we hope to exploit is that Ψ is a single-valued function of θ only, $\Psi \equiv \Psi(\theta)$. The moisture potential for the GDL plays a central role in the performance of the fuel cell. While we understand that the GDL has not been characterized, our efforts here to model Ψ with a small number of parameters may help guide design and characterization efforts.

To simplify our system, we assume that θ represents the liquid water volumetric fraction, and that the vapor content is always in thermodynamic equilibrium and fully saturated. We justify this assumption with the fact that the membrane is thin and that the channels supplying oxygen and other gases are known to be fully saturated.

Knowing that water is virtually incompressible, one may write

$$\nabla \cdot [D_\theta(\theta)\nabla\theta] + \Sigma = 0, \tag{2.2a}$$

where Σ represents any sources and sinks of water due to evaporation and condensation, and D_θ, the diffusion coefficient of water, is given by

$$D_\theta(\theta) = \kappa_\theta(\theta)\frac{d\Psi}{d\theta}. \tag{2.2b}$$

Again, the specific form of D must come from a material characterization of the GDL, but we considered two alternatives. The first attempt to capture the right general behavior over all θ is strongly motivated by measurements of clays [9, 11]:

$$D_\theta(\theta) = A\exp\left\{-B\left[\cot\left(\pi W\right)\right]^p\right\}, \tag{2.3a}$$

where A, B, and p are material parameters, and $W = \theta/\phi$ is the pore volume concentration of water. The important feature is that $D_\theta(0) = 0$, and $D_\theta(\theta) \to \infty$ as $W \to 1$. Since we are trying to focus on the regime where θ is bounded away from ϕ, the following model takes into account the other behavior more simply:

$$D_\theta(\theta) = A\left(1 - e^{-B\theta}\right)^p. \tag{2.3b}$$

For the gases, we include both Fickian diffusion and convection for the transport. Thus we have

$$\nabla\cdot\left(D_u(\theta)\nabla\tilde{u} - \tilde{u}\tilde{\mathbf{V}}_{\mathrm{g}}\right) = 0, \tag{2.4}$$

where $\tilde{\mathbf{V}}_{\mathrm{g}}$ is the velocity of the gas phase and D_u is the diffusion coefficient of oxygen. In (2.4) (and throughout this section), we assume that the diffusion properties of the gas diffusion layer are spatially uniform. In reality, the gas diffusion layer is made up of fibers parallel to the $\tilde{x}$-axis. This enhances diffusion in the $\tilde{x}$-direction, thus negating the favorable properties of the small aspect ratio.

Evaporation is temperature-dependent process with an Arrhenius law, so we have

$$\text{evaporation term} \propto \exp\left(-\frac{E_{\mathrm{A}}}{R\tilde{T}}\right)\theta, \tag{2.5a}$$

where E_{A} is the activation energy and R is the gas constant. However, it will be shown that the variations in temperature are quite small, so it may be appropriate to treat the exponential as a constant. Hence one may use

$$\text{evaporation term} \propto \theta. \tag{2.5b}$$

Note that if there is no liquid water ($\theta = 0$), there will be no evaporation.

Similarly, there will be condensation, but this is not a temperature-dependent process. Thus we have

$$\text{condensation term} \propto \tilde{v}. \tag{2.6}$$

Note that if there is no water vapor ($\tilde{v} = 0$), there will be no condensation. Then using these forms to track the volume fraction of water, so we have

$$\nabla\cdot\left(D_\theta(\theta)\nabla\theta\right) - \beta_\theta\exp\left(-\frac{E_{\mathrm{A}}}{R\tilde{T}}\right)\theta + \beta_v\tilde{v} = 0, \tag{2.7}$$

where the βs are conversion factors. Note that the evaporation term removes water (minus sign), while the condensation term produces it (plus sign).

Earlier, we proposed assuming the gas was fully saturated with water so that $\tilde{v}$ could be specified. However, we can model the vapor transport as well. Tracking the evolution of the vapor phase of water, we must also include convection. Thus, we have

$$\nabla \cdot (D_v(\theta)\nabla\tilde{v} - \tilde{v}\tilde{\mathbf{V}}_{\mathrm{g}}) + v_{\mathrm{l}}\left[\beta_\theta \exp\left(-\frac{E_{\mathrm{A}}}{R\tilde{T}}\right)\theta - \beta_v\tilde{v}\right] = 0, \tag{2.8}$$

where D_v is the diffusion coefficient of the water vapor and v_{l} is a normalization factor defined below. Note that the evaporation term produces vapor (plus sign), while the condensation term removes it (minus sign).

For the temperature, we use convection and Fourier's Law for heat conduction, supplemented by a heat gain (for condensation) and loss (evaporation). Since the gas and liquid water velocities are small, we assume that thermal transport from water and gas movement is so small as to be neglected. Thus we have

$$\nabla \cdot (\tilde{k}(\theta)\nabla\tilde{T}) - \rho_\theta L\left[\beta_\theta \exp\left(-\frac{E_{\mathrm{A}}}{R\tilde{T}}\right)\theta - \beta_v\tilde{v}\right] = 0, \tag{2.9}$$

where $\tilde{k}$ is the thermal conductivity, ρ_θ is the density of liquid water, and L is the latent heat. Note that the evaporation term uses up heat (minus sign), while the condensation term produces it (plus sign).

To model $\tilde{k}(\theta)$ in the presence of liquid water, we choose a linear interpolation:

$$\tilde{k}(\theta) = \tilde{k}_{\mathrm{C}} + \tilde{k}_\theta\theta, \tag{2.10}$$

where $\tilde{k}_{\mathrm{C}}$ is the thermal conductivity of the dry (graphite) GDL and $\tilde{k}_\theta$ is the thermal conductivity of water.

If the gas phase actually convects, the velocity is governed by Darcy's Law:

$$\tilde{\mathbf{V}}_{\mathrm{g}} = -\frac{\kappa_{\mathrm{g}}(\theta)}{\mu}\nabla\tilde{P}, \tag{2.11}$$

where κ_{g} is the permeability of the GDL to gases and μ is the viscosity of the gas. The permeability κ_{g} depends upon θ because liquid water will remove available pore space for the gas. To solve for the pressure, we use the continuity equation:

$$\nabla \cdot \tilde{\mathbf{V}}_{\mathrm{g}} = -\frac{1}{\mu}\nabla \cdot (\kappa_{\mathrm{g}}(\theta)\nabla\tilde{P}) = 0. \tag{2.12}$$

Another possibility is to let the mass fraction of water be represented by a single variable. Then this variable would be small in regions where there is mostly water vapor, and high where there is mostly liquid water. Philip & De Vries explore this thoroughly in [10]. The resulting system would yield a moisture transport equation driven by thermal and hydraulic gradients rather than just the latter, and equation (2.8) can be discarded

entirely. However, as Philip & De Vries note in their 1957 paper, the thermal gradient diffusivity term in the hydraulic transport equation is several orders of magnitude less than the liquid gradient diffusivity [10].

Clearly, the transport and evolution of each of the variables (vapor, liquid water, heat and gas) requires careful attention. Yet consideration of all at once will yield a complex system that provides little physical insight. Given that the GDL is just a small part of a larger more complex system, the crucial issue is to determine what interdependencies exist. The workshop team opted to divide into a small number of squads, each making strong assumptions to see what could be learned if the behavior of the GDL were dominated by one of these regimes. For instance, one team focused on gas and heat transport assuming the GDL was completely dry. Another focused on the interdiffusion of two distinct gas phases within a dry GDL. The third squad examined hydrothermal transport as a function of the material properties of the GDL, assuming that gas transport in the matrix would have little or no impact on the formation of liquid water.

Moving on to geometric considerations and boundary conditions, the boundary $\tilde{y} = h$, $|\tilde{x}| \leq d$ is the solid graphite cathode. For reasons that will become clear later, we denote quantities in the *middle* of the GDL ($|\tilde{x}| \leq d$) by sub- or superscripts "m". (If a dependent variable appears without superscripts, one should assume the equation holds throughout the GDL.) By assuming high thermal conductivity of the interface, we may replace the standard radiation condition by an imposed temperature:

$$\tilde{T}^{\mathrm{m}}(\tilde{x}, h) = T_{\mathrm{m}}, \qquad |\tilde{x}| < d. \tag{2.13}$$

The wall is impermeable, so we have

$$\frac{\partial \tilde{u}^{\mathrm{m}}}{\partial \tilde{y}}(\tilde{x}, h) = \frac{\partial \tilde{v}^{\mathrm{m}}}{\partial \tilde{y}}(\tilde{x}, h) = \frac{\partial \tilde{P}^{\mathrm{m}}}{\partial \tilde{y}}(\tilde{x}, h) = \frac{\partial \tilde{\theta}^{\mathrm{m}}}{\partial \tilde{y}}(\tilde{x}, h) = 0, \qquad |\tilde{x}| < d. \tag{2.14}$$

The boundaries $\tilde{y} = h$, $-2d \leq \tilde{x} \leq -d$ and $d \leq \tilde{x} \leq 2d$ represent the exposed left and right channels, respectively, so we use sub- and superscripts "l" and "r". By assuming high permeability of the interface, we may replace the standard radiation conditions by imposed function values. Lastly, we assume that there is no liquid water at the exposed interface. We begin by listing the equations on the left:

$$\tilde{u}^{\mathrm{l}}(\tilde{x}, h) = u_{\mathrm{l}}, \qquad -2d \leq \tilde{x} \leq -d, \tag{2.15a}$$
$$\tilde{T}^{\mathrm{l}}(\tilde{x}, h) = T_{\mathrm{l}}, \qquad -2d \leq \tilde{x} \leq -d, \tag{2.15b}$$
$$\tilde{v}^{\mathrm{l}}(\tilde{x}, h) = v_{\mathrm{l}}, \qquad -2d \leq \tilde{x} \leq -d, \tag{2.15c}$$
$$\tilde{P}^{\mathrm{l}}(\tilde{x}, h) = P_{\mathrm{l}}, \qquad -2d \leq \tilde{x} \leq -d, \tag{2.15d}$$
$$\theta^{\mathrm{l}}(\tilde{x}, h) = 0, \qquad -2d \leq \tilde{x} \leq -d. \tag{2.15e}$$

Here $T_{\mathrm{l}} > T_{\mathrm{m}}$. There may also be some adjustments necessary to compensate for the porosity of the GDL.

The temperature in the channel on the right is the same as the channel on the left, so we have

$$\tilde{T}^{\mathrm{r}}(\tilde{x}, h) = T_{\mathrm{l}}, \qquad d \leq \tilde{x} \leq 2d. \tag{2.16a}$$

The pressure in the right channel is given by

$$\tilde{P}^{\mathrm{r}}(\tilde{x},h) = P_{\mathrm{r}}, \qquad d \le \tilde{x} \le 2d, \tag{2.16b}$$

where $P_{\mathrm{r}} \le P_{\mathrm{l}}$. The gas concentrations in the channels are proportional to the total pressure *via* the ideal gas law $\tilde{P} = \tilde{u}R\tilde{T}$ (for example). Thus we have

$$\begin{aligned} \tilde{u}^{\mathrm{r}}(\tilde{x},h) &= \frac{P_{\mathrm{r}}}{P_{\mathrm{l}}}u_{\mathrm{l}}, \qquad d \le \tilde{x} \le 2d \\ &= u_{\mathrm{l}}(1-\gamma\epsilon^2), \qquad \gamma\epsilon^2 = \frac{P_{\mathrm{l}}-P_{\mathrm{r}}}{P_{\mathrm{l}}} \end{aligned} \tag{2.16c}$$

$$\tilde{v}^{\mathrm{r}}(\tilde{x},h) = v_{\mathrm{l}}(1-\gamma\epsilon^2), \qquad d \le \tilde{x} \le 2d, \tag{2.16d}$$

where the choice of the size of r is motivated by Appendix A. Again, we assume that no liquid water exists in the channel:

$$\theta^{\mathrm{r}}(\tilde{x},h) = 0, \qquad d \le \tilde{x} \le 2d. \tag{2.16e}$$

Since our GDL block is periodic, we must have no-flux conditions at $\tilde{x} = \pm 2d$:

$$\frac{\partial\tilde{u}^{\mathrm{l}}}{\partial\tilde{x}}(-2d,\tilde{y}) = \frac{\partial\tilde{T}^{\mathrm{l}}}{\partial\tilde{x}}(-2d,\tilde{y}) = \frac{\partial\tilde{v}^{\mathrm{l}}}{\partial\tilde{x}}(-2d,\tilde{y}) = \frac{\partial\tilde{P}^{\mathrm{l}}}{\partial\tilde{x}}(-2d,\tilde{y}) = \frac{\partial\theta^{\mathrm{l}}}{\partial\tilde{x}}(-2d,\tilde{y}) = 0, \tag{2.17}$$

$$\frac{\partial\tilde{u}^{\mathrm{r}}}{\partial\tilde{x}}(2d,\tilde{y}) = \frac{\partial\tilde{T}^{\mathrm{r}}}{\partial\tilde{x}}(2d,\tilde{y}) = \frac{\partial\tilde{v}^{\mathrm{r}}}{\partial\tilde{x}}(2d,\tilde{y}) = \frac{\partial\tilde{P}^{\mathrm{r}}}{\partial\tilde{x}}(2d,\tilde{y}) = \frac{\partial\theta^{\mathrm{r}}}{\partial\tilde{x}}(2d,\tilde{y}) = 0. \tag{2.18}$$

At the bottom of the GDL, the pressure gradient is zero:

$$\frac{\partial\tilde{P}}{\partial\tilde{y}}(\tilde{x},0) = 0. \tag{2.19a}$$

In addition, we assume that no liquid water forms at the bottom:

$$\theta(\tilde{x},0) = 0. \tag{2.19b}$$

Flux conditions on $\tilde{T}$, $\tilde{u}$, and $\tilde{v}$ vary with the specific model and will be presented later.

Section 3: No Liquid: Governing Equations

As a first approximation, we neglect the liquid water in the gas diffusion layer, as well as the possibilty of condensation. The idea is to examine $\tilde{T}$ and $\tilde{v}$ to check the concentration at each point. In [3] the authors define the saturation concentration of water vapor *via* the pressure as follows:

$$\log_{10}(\tilde{P}_{\text{sat}}) = -2.18 + 0.029(\tilde{T} - 273.2) - 9.18 \times 10^{-5}(\tilde{T} - 273.2)^2 + 1.44 \times 10^{-7}(\tilde{T} - 273.2)^3.$$

Here pressure is assumed to be measured in atmospheres, and $\tilde{T}$ in K. Using the ideal gas law $\tilde{P} = \tilde{v}R\tilde{T}$, we have

$$\begin{aligned} \tilde{v}_{\text{sat}} R\tilde{T} &= 10^{\left(-2.18+0.029(\tilde{T}-273.2)-9.18\times10^{-5}(\tilde{T}-273.2)^2+1.44\times10^{-7}(\tilde{T}-273.2)^3\right)} \\ \tilde{v}_{\text{sat}}(\tilde{T}) &= \frac{1}{R\tilde{T}} \exp\left(-45.8 + (2.565 \times 10^{-1})\tilde{T} - 4.831 \times 10^{-4}\tilde{T}^2 + 3.316 \times 10^{-7}\tilde{T}^3\right). \end{aligned} \tag{3.1}$$

If $\tilde{v} > \tilde{v}_{\text{sat}}$ in some area, then condensation occurs and the model fails. But perhaps we can obtain bounds on the temperature regimes necessary to produce condensation.

With no water, all of our nonlinear parameters in section 2 become constant. Also, our evaporation and condensation terms become meaningless. Thus (2.12) and (2.4) become

$$\begin{aligned} \frac{\kappa_{\text{g}}}{\mu}\left(\frac{\partial^2\tilde{P}}{\partial\tilde{x}^2} + \frac{\partial^2\tilde{P}}{\partial\tilde{y}^2}\right) &= 0 \\ \nabla^2\tilde{P} = \frac{\partial^2\tilde{P}}{\partial\tilde{x}^2} + \frac{\partial^2\tilde{P}}{\partial\tilde{y}^2} &= 0, \\ D_u\left(\frac{\partial^2\tilde{u}}{\partial\tilde{x}^2} + \frac{\partial^2\tilde{u}}{\partial\tilde{y}^2}\right) - \nabla\cdot(\tilde{u}\tilde{\mathbf{V}}_{\text{g}}) &= 0 \\ D_u\left(\frac{\partial^2\tilde{u}}{\partial\tilde{x}^2} + \frac{\partial^2\tilde{u}}{\partial\tilde{y}^2}\right) + \frac{\kappa_{\text{g}}}{\mu}\nabla\cdot(\tilde{u}\nabla\tilde{P}) &= 0 \\ \frac{\partial^2\tilde{u}}{\partial\tilde{x}^2} + \frac{\partial^2\tilde{u}}{\partial\tilde{y}^2} + \frac{\kappa_{\text{g}}}{\mu D_u}(\nabla\tilde{u}\cdot\nabla\tilde{P} + u\nabla^2\tilde{P}) &= 0, \end{aligned} \tag{3.2}$$

where we have used (2.11). Then using (3.2) to simplify the above equation, we have

$$\frac{\partial^2\tilde{u}}{\partial\tilde{x}^2} + \frac{\partial^2\tilde{u}}{\partial\tilde{y}^2} + \frac{\kappa_{\text{g}}}{\mu D_u}\left[\left(\frac{\partial\tilde{u}}{\partial\tilde{x}}\right)\left(\frac{\partial\tilde{P}}{\partial\tilde{x}}\right) + \left(\frac{\partial\tilde{u}}{\partial\tilde{y}}\right)\left(\frac{\partial\tilde{P}}{\partial\tilde{y}}\right)\right] = 0. \tag{3.3}$$

Because of the similarities between (2.4) and (2.8) we see that (2.8) becomes

$$\frac{\partial^2\tilde{v}}{\partial\tilde{x}^2} + \frac{\partial^2\tilde{v}}{\partial\tilde{y}^2} + \frac{\kappa_{\text{g}}}{\mu D_v}\left[\left(\frac{\partial\tilde{v}}{\partial\tilde{x}}\right)\left(\frac{\partial\tilde{P}}{\partial\tilde{x}}\right) + \left(\frac{\partial\tilde{v}}{\partial\tilde{y}}\right)\left(\frac{\partial\tilde{P}}{\partial\tilde{y}}\right)\right] = 0. \tag{3.4}$$

With the convection neglected in (2.9), our expression becomes much simpler:

$$\frac{\partial^2 \tilde{T}}{\partial \tilde{x}^2} + \frac{\partial^2 \tilde{T}}{\partial \tilde{y}^2} = 0. \tag{3.5}$$

The governing equations and boundary conditions motivate the following scalings:

$$x = \frac{\tilde{x}}{d}, \qquad y = \frac{\tilde{y}}{h}, \qquad T(x,y) = \frac{\tilde{T}(\tilde{x},\tilde{y}) - T_{\mathrm{m}}}{T_{\mathrm{l}} - T_{\mathrm{m}}}, \qquad u = \frac{\tilde{u}}{u_{\mathrm{l}}}, \qquad v = \frac{\tilde{v}}{v_{\mathrm{l}}}, \tag{3.6a}$$

$$P(x,y) = \frac{2\tilde{P}(\tilde{x},\tilde{y}) - (P_{\mathrm{l}} + P_{\mathrm{r}})}{P_{\mathrm{l}} - P_{\mathrm{r}}}. \tag{3.6b}$$

Substituting (3.6) into (3.2) and (3.3), we obtain

$$\begin{aligned} \frac{P_{\mathrm{l}} - P_{\mathrm{r}}}{2d^2}\frac{\partial^2 P}{\partial x^2} + \frac{P_{\mathrm{l}} - P_{\mathrm{r}}}{2h^2}\frac{\partial^2 P}{\partial y^2} &= 0 \\ \epsilon^2 \frac{\partial^2 P}{\partial x^2} + \frac{\partial^2 P}{\partial y^2} &= 0. \end{aligned} \tag{3.7}$$

$$\begin{aligned} u_{\mathrm{l}}\left(\frac{1}{d^2}\frac{\partial^2 u}{\partial x^2} + \frac{1}{h^2}\frac{\partial^2 u}{\partial y^2}\right) + \frac{\kappa_{\mathrm{g}} u_{\mathrm{l}}(P_{\mathrm{l}} - P_{\mathrm{r}})}{2\mu D_u}\left[\frac{1}{d^2}\left(\frac{\partial u}{\partial x}\right)\left(\frac{\partial P}{\partial x}\right) + \frac{1}{h^2}\left(\frac{\partial u}{\partial y}\right)\left(\frac{\partial P}{\partial y}\right)\right] &= 0 \\ \epsilon^2 \frac{\partial^2 u}{\partial x^2} + \frac{\partial^2 u}{\partial y^2} + \mathrm{Pe}_u\left[\epsilon^2\left(\frac{\partial u}{\partial x}\right)\left(\frac{\partial P}{\partial x}\right) + \left(\frac{\partial u}{\partial y}\right)\left(\frac{\partial P}{\partial y}\right)\right] &= 0, \end{aligned} \tag{3.8a}$$

$$\mathrm{Pe}_u = \frac{\kappa_{\mathrm{g}}(P_{\mathrm{l}} - P_{\mathrm{r}})}{2\mu D_u}, \tag{3.8b}$$

where Pe_u is the Péclet number for the oxygen. Since (3.4) is simply (3.3) with v replacing u, we have

$$\epsilon^2 \frac{\partial^2 v}{\partial x^2} + \frac{\partial^2 v}{\partial y^2} + \mathrm{Pe}_v\left[\epsilon^2\left(\frac{\partial v}{\partial x}\right)\left(\frac{\partial P}{\partial x}\right) + \left(\frac{\partial v}{\partial y}\right)\left(\frac{\partial P}{\partial y}\right)\right] = 0, \qquad \mathrm{Pe}_v = \frac{\kappa_{\mathrm{g}}(P_{\mathrm{l}} - P_{\mathrm{r}})}{2\mu D_v}. \tag{3.9}$$

Substituting (3.6) into (3.5), we have

$$\epsilon^2 \frac{\partial^2 T}{\partial x^2} + \frac{\partial^2 T}{\partial y^2} = 0. \tag{3.10}$$

Next we substitute our scalings into our boundary conditions (2.13)–(2.19) and rearrange by dependent variable. Since the pressure conditions do not become important until

section 6, we examine only the remaining dependent variables. For the temperature, we have

$$(T_\mathrm{l} - T_\mathrm{m})T^\mathrm{m}(x,1) + T_\mathrm{m} = T_\mathrm{m}, \qquad |x| < 1,$$
$$T^\mathrm{m}(x,1) = 0, \tag{3.11a}$$
$$(T_\mathrm{l} - T_\mathrm{m})T^\mathrm{l}(x,1) + T_\mathrm{m} = T_\mathrm{l}, \qquad -2 \le x \le -1$$
$$T^\mathrm{l}(x,1) = 1, \tag{3.11b}$$
$$(T_\mathrm{l} - T_\mathrm{m})T^\mathrm{r}(x,1) + T_\mathrm{m} = T_\mathrm{l} \qquad 1 \le x \le 2$$
$$T^\mathrm{r}(x,1) = 1, \tag{3.11c}$$
$$\frac{\partial T^\mathrm{l}}{\partial x}(-2,y) = 0, \tag{3.12a}$$
$$\frac{\partial T^\mathrm{r}}{\partial x}(2,y) = 0. \tag{3.12b}$$

For the oxygen, we have

$$\frac{\partial u^\mathrm{m}}{\partial y}(x,1) = 0, \qquad |x| < 1, \tag{3.13a}$$
$$u_\mathrm{l} u^\mathrm{l}(x,1) = u_\mathrm{l}, \qquad -2 \le x \le -1$$
$$u^\mathrm{l}(x,1) = 1, \tag{3.13b}$$
$$u_\mathrm{l} u^r(x,1) = u_\mathrm{l}(1 - \gamma\epsilon^2), \qquad 1 \le x \le 2$$
$$u^\mathrm{r}(x,1) = 1 - \gamma\epsilon^2, \tag{3.13c}$$
$$\frac{\partial u^\mathrm{l}}{\partial x}(-2,y) = 0, \tag{3.14a}$$
$$\frac{\partial u^\mathrm{r}}{\partial x}(2,y) = 0. \tag{3.14b}$$

For the water vapor, we have

$$\frac{\partial v^\mathrm{m}}{\partial y}(x,1) = 0, \qquad |x| < 1, \tag{3.15a}$$
$$v_\mathrm{l} v^\mathrm{l}(x,1) = v_\mathrm{l}, \qquad -2 \le x \le -1$$
$$v^\mathrm{l}(x,1) = 1, \tag{3.15b}$$
$$v_\mathrm{l} v^r(x,1) = v_\mathrm{l}(1 - \gamma\epsilon^2), \qquad 1 \le x \le 2$$
$$v^\mathrm{r}(x,1) = 1 - \gamma\epsilon^2, \tag{3.15c}$$
$$\frac{\partial v^\mathrm{l}}{\partial x}(-2,y) = 0, \tag{3.16a}$$
$$\frac{\partial v^\mathrm{r}}{\partial x}(2,y) = 0. \tag{3.16b}$$

Lastly, we substitute our scalings into our saturation equation (3.1) to obtain

$$v_\mathrm{l} v_\mathrm{sat} = \frac{1}{R[(T_\mathrm{l} - T_\mathrm{m})T + T_\mathrm{m}]} \exp\left(-45.8 + (2.565 \times 10^{-1})[(T_\mathrm{l} - T_\mathrm{m})T + T_\mathrm{m}]\right.$$

$$-4.831\times10^{-4}[(T_\mathrm{l}-T_\mathrm{m})T+T_\mathrm{m}]^2+(3.316\times10^{-7})[(T_\mathrm{l}-T_\mathrm{m})T+T_\mathrm{m}]^3\big)\,.$$

$$v_\mathrm{sat}(T)=\frac{1}{Rv_\mathrm{l}[(T_\mathrm{l}-T_\mathrm{m})T+T_\mathrm{m}]}\exp\big(-45.8+(2.565\times10^{-1})[(T_\mathrm{l}-T_\mathrm{m})T+T_\mathrm{m}]$$
$$-4.831\times10^{-4}[(T_\mathrm{l}-T_\mathrm{m})T+T_\mathrm{m}]^2+(3.316\times10^{-7})[(T_\mathrm{l}-T_\mathrm{m})T+T_\mathrm{m}]^3\big)\,. \quad (3.17)$$

Again, all units should be stripped from dimensional quantities when using this formula. Substituting our parameters from Appendix A into the above, we have

$$v_\mathrm{sat}=\frac{1}{(82.05)(1.72\times10^{-5})(2T+353)}\exp\big(-45.8+(2.565\times10^{-1})(2T+353)$$
$$-4.831\times10^{-4}(2T+353)^2+(3.316\times10^{-7})(2T+353)^3\big)\,.$$

$$v_\mathrm{sat}(T)=\frac{710}{2T+353}\exp\big(-0.869+(7.87\times10^{-2})T-(5.28\times10^{-4})T^2+(2.65\times10^{-6})T^3\big)\,. \quad (3.18)$$

Section 4: No Liquid, No Convection, Constant Flux

As a first attempt, we assume that the pressure is constant. Thus the transport is Fickian only, and (3.8a), (3.9), and (3.10) become

$$\epsilon^2 \frac{\partial^2 u}{\partial x^2} + \frac{\partial^2 u}{\partial y^2} = 0, \tag{4.1}$$

$$\epsilon^2 \frac{\partial^2 v}{\partial x^2} + \frac{\partial^2 v}{\partial y^2} = 0, \tag{4.2}$$

$$\epsilon^2 \frac{\partial^2 T}{\partial x^2} + \frac{\partial^2 T}{\partial y^2} = 0. \tag{4.3}$$

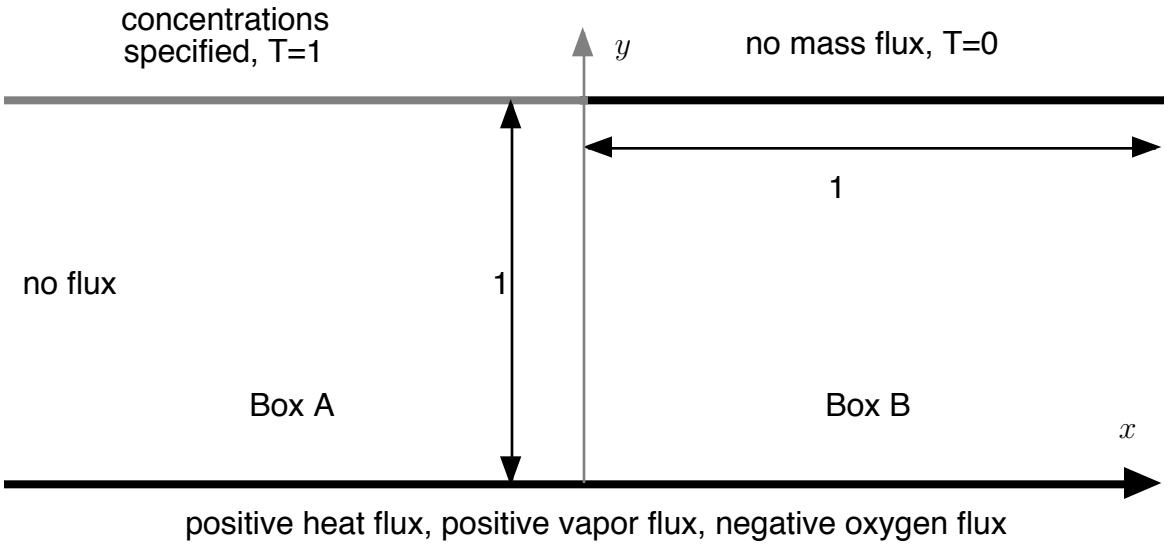

Figure 4.1. Schematic of geometry for convection-free problem.

Upon examination of our boundary conditions (3.11)–(3.16) we see that with a constant pressure, the regions of positive and negative x are symmetric about $x = 0$. For historical reasons, we restrict our attention to the region $-2 \le x \le 0$. Thus we can replace the boundary conditions on the "r" variables with the following:

$$\frac{\partial T^{\mathrm{m}}}{\partial x}(0, y) = 0, \tag{4.4a}$$

$$\frac{\partial u^{\mathrm{m}}}{\partial x}(0, y) = 0, \tag{4.4b}$$

$$\frac{\partial v^{\mathrm{m}}}{\partial x}(0, y) = 0. \tag{4.4c}$$

There are several types of conditions one can impose at the interface with the CCL ($\tilde{y} = 0$). For now we impose fluxes for each of our quantities of interest. As an initial model, we assume constant flux. Oxygen flows out of the gas diffusion layer, so

$$\text{oxygen flux} = D_u \frac{\partial \tilde{u}}{\partial n} = -D_u \frac{\partial \tilde{u}}{\partial \tilde{y}}(\tilde{x}, 0) = -\tilde{q}_u$$
$$D_u \frac{\partial \tilde{u}}{\partial \tilde{y}}(\tilde{x}, 0) = \tilde{q}_u. \tag{4.5a}$$

Here we have chosen the sign such that $\tilde{q}_u \geq 0$. Since the sign of the gradient is the opposite of the sign of the flux, the water vapor and temperature fluxes are given by

$$D_v \frac{\partial \tilde{v}}{\partial \tilde{y}}(\tilde{x}, 0) = -\tilde{q}_v, \tag{4.5b}$$

$$\tilde{k}_{\mathrm{C}} \frac{\partial \tilde{T}}{\partial \tilde{y}}(\tilde{x}, 0) = -\tilde{q}_T, \tag{4.5c}$$

where we retain the convention of keep the $\tilde{q}$s positive.

Substituting (3.6) into (4.5), we have the following:

$$D_u \frac{u_{\mathrm{l}}}{h} \frac{\partial u}{\partial y}(x, 0) = \tilde{q}_u$$
$$\frac{\partial u}{\partial y}(x, 0) = q_u \epsilon^2, \qquad q_u \epsilon^2 = \frac{\tilde{q}_u h}{D_u u_{\mathrm{l}}}, \tag{4.6a}$$

$$D_v \frac{v_{\mathrm{l}}}{h} \frac{\partial v}{\partial y}(x, 0) = -\tilde{q}_v$$
$$\frac{\partial v}{\partial y}(x, 0) = -q_v \epsilon^2, \qquad q_v \epsilon^2 = \frac{\tilde{q}_v h}{D_v v_{\mathrm{l}}}, \tag{4.6b}$$

$$\tilde{k}_{\mathrm{C}} \frac{T_{\mathrm{l}} - T_{\mathrm{m}}}{h} \frac{\partial T}{\partial y}(x, 0) = -\tilde{q}_T$$
$$\frac{\partial T}{\partial y}(x, 0) = -q_T, \qquad q_T = \frac{\tilde{q}_T h}{\tilde{k}_{\mathrm{C}}(T_{\mathrm{l}} - T_{\mathrm{m}})}. \tag{4.6c}$$

Here the qs are the Nusselt numbers. In (4.6a) and (4.6b) we have added the factor ϵ^2, which is consistent with the size given in Appendix A, for later computational convenience.

Since $\epsilon = 0.2$, as a first approximation we use it as a perturbation parameter. Thus we expand our dependent variables in the following series:

$$T(x, y; \epsilon) = T_0(x, y) + o(\epsilon), \tag{4.7a}$$
$$u(x, y; \epsilon) = u_0(x, y) + o(\epsilon), \tag{4.7b}$$
$$v(x, y; \epsilon) = v_0(x, y) + o(\epsilon). \tag{4.7c}$$

We begin by examining the temperature field. Substituting (4.7a) into (4.3), we obtain, to leading order,

$$\frac{\partial^2 T_0}{\partial y^2} = 0. \tag{4.8}$$

To leading order, all the other boundary conditions for T hold with T replaced by T_0. Integrating (4.8) subject to (3.12a), (4.4a) and (4.6c), we have

$$\frac{\partial T_0}{\partial y} = -q_T$$
$$T_0 = -q_T y + f(x), \qquad f'(-2) = f'(0) = 0.$$

Since the boundary conditions in (3.11a) and (3.11b) are different depending on the region, we break our solution into two parts, obtaining

$$T_0^{\mathrm{l}}(x,y) = q_T(1-y) + 1, \qquad -2 \le x \le -1, \tag{4.9a}$$
$$T_0^{\mathrm{m}}(x,y) = q_T(1-y), \qquad -1 \le x \le 0. \tag{4.9b}$$

Laplace's equation cannot support the discontinuity at $x = 0$, so we introduce the interior layer variables

$$z = \frac{x+1}{\epsilon}, \qquad T(x,y) = q_T(1-y) + T^{\mathrm{i}}(z,y), \tag{4.10}$$

where the superscript "i" refers to "interior". Substituting (4.10) into (4.3), (4.6c), (3.11a), and (3.11b), we obtain, to leading order,

$$\frac{\partial^2 T^{\mathrm{i}}}{\partial z^2} + \frac{\partial^2 T^{\mathrm{i}}}{\partial y^2} = 0 \tag{4.11}$$
$$-q_T + \frac{\partial T^{\mathrm{i}}}{\partial y}(z,0) = -q_T$$
$$\frac{\partial T^{\mathrm{i}}}{\partial y}(z,0) = 0, \tag{4.12}$$
$$T^{\mathrm{i}}(z,1) = 1, \qquad z < 0 \tag{4.13a}$$
$$T^{\mathrm{i}}(z,1) = 0, \qquad z > 0. \tag{4.13b}$$

The remaining conditions are given by matching to the outer solutions:

$$q_T(1-y) + T^{\mathrm{i}}(-\infty, y) = T^{\mathrm{l}}\left(-1^-, y\right) = q_T(1-y) + 1$$
$$T^{\mathrm{i}}(-\infty, y) = 1, \tag{4.14a}$$
$$q_T(1-y) + T^{\mathrm{i}}(\infty, y) = T^{\mathrm{m}}\left(-1^+, y\right) = q_T(1-y)$$
$$T^{\mathrm{i}}(\infty, y) = 0. \tag{4.14b}$$

The system (4.11)–(4.14) is essentially a potential problem in an infinite strip. The full solution can be written down using conformal mapping techniques.

Figure 4.2 shows a contour plot of the temperature using the full equation (4.3) and the parameters in Appendix A. The solution was computed using Matlab. Here (and in all such plots) the domain has been shifted slightly; $-1 \le x \le 0$ is the left region, and $0 \le x \le 1$ is the middle region.

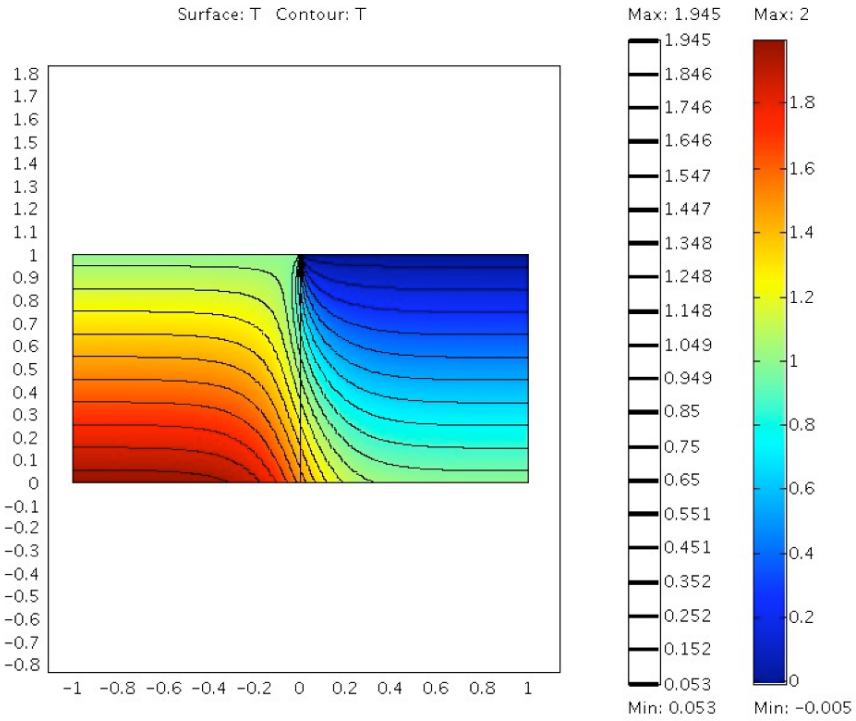

Figure 4.2. Contour plot of temperature.

Note the nearly horizontal contours in the outer regions, showing that the temperature is very nearly a function of y only. Also note that the difference between the temperature on the left and right (for the same value of y) is very nearly 1. Because our value for ϵ is 0.2, the interior layer behavior is smeared out a bit.

If we let $f_1 = z + iy$, then the chain of transformations

$$f_2 = \exp(\pi f_1), \qquad f_3 = \frac{f_2 - 1}{f_2 + 1}, \qquad f_4 = \frac{1}{2} + \frac{1}{\pi}\sin^{-1}(f_3)$$

maps the infinite strip of (4.11)–(4.13) to the interior of a half-strip in the f_4-plane, such that $\{y = 0\}$ maps to the real interval $(0, 1)$, $\{y = 1, z > 0\}$ maps to the positive real axis, and $\{y = 1, z < 0\}$ maps to $\{\Re f_4 = 1, \Im f_4 > 0\}$. Therefore, by the conformal invariance of Laplace's equation and the boundary conditions, $T^{\mathrm{i}} = \Re f_4$ is the solution of (4.11)–(4.13). This function is plotted in Figure 4.3 using Matlab.

We continue on with a discussion of the gas profiles, beginning with u. (The discussion for v is directly analogous.) If we proceed as above, substituting (4.7b) into (4.1) yields, to leading order,

$$\frac{\partial^2 u_0}{\partial y^2} = 0. \tag{4.15}$$

Again, all the other conditions remain the same with u replaced by u_0. We must make a special explanation for (4.6a), which for the left region we leave in the form

$$\frac{\partial u^{\mathrm{l}}}{\partial y}(x, 0) = q_u \epsilon^2. \tag{4.16}$$

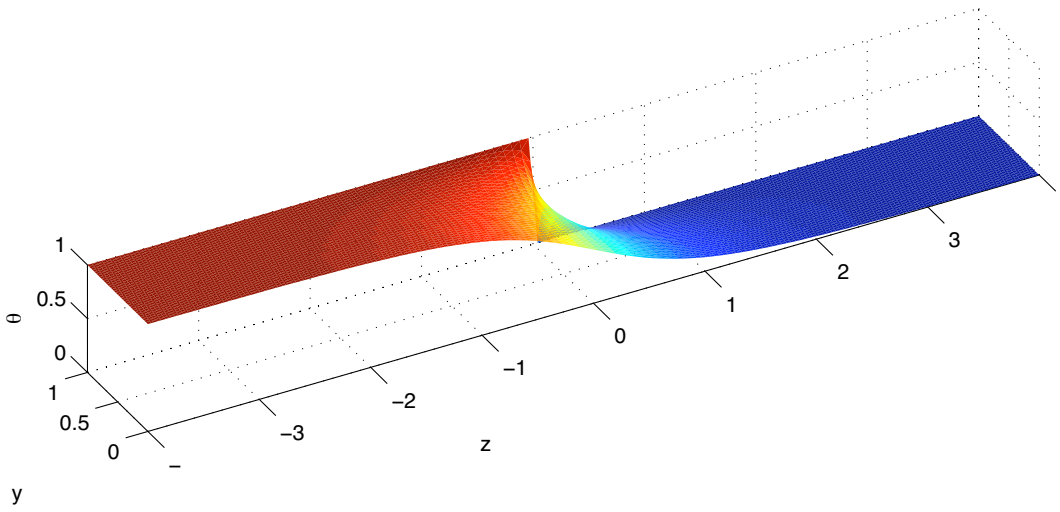

Figure 4.3. 3-D plot of T^{i} in interior layer.

We note that technically we should have pushed the right-hand side of (4.16) to a lower order. However, we can solve the leading-order problem as stated without resorting to a perturbation series for (4.16), and so we leave it as is.

Proceeding as above, integrating (4.15) once we have

$$\frac{\partial u_0}{\partial y} = f(x). \tag{4.17}$$

We may solve (4.17) subject to (3.13b), (3.14a), and (4.16) to obtain

$$u^{\mathrm{l}}(x,y) = 1 - q_u\epsilon^2(1-y), \qquad -2 \le x \le -1. \tag{4.18}$$

However, in the middle we see that (3.13a) along with the full boundary condition (4.16) makes the problem ill-posed. Therefore, in that region we do split up equation (4.16) and assume the following expansion:

$$u^{\mathrm{m}}(x,y;\epsilon) = u_0^{\mathrm{m}}(x,y) + \epsilon^2 u_2^{\mathrm{m}}(x,y) + o(1), \qquad -1 \le x \le 0. \tag{4.19}$$

Substituting (4.19) into (4.1) and (4.6a), we obtain, to leading orders,

$$\epsilon^2\frac{\partial^2(u_0^{\mathrm{m}}+u_2^{\mathrm{m}})}{\partial x^2} + \frac{\partial^2(u_0^{\mathrm{m}}+u_2^{\mathrm{m}})}{\partial y^2} = 0$$

$$\frac{\partial^2 u_0^{\mathrm{m}}}{\partial y^2} = 0, \tag{4.20a}$$

$$\frac{\partial^2 u_2^{\mathrm{m}}}{\partial y^2} = -\frac{\partial^2 u_0^{\mathrm{m}}}{\partial x^2}, \tag{4.20b}$$

$$\frac{\partial u_0^{\mathrm{m}}}{\partial y}(x,0) = 0, \tag{4.21a}$$

$$\frac{\partial u_2^{\mathrm{m}}}{\partial y}(x,0) = q_u. \tag{4.21b}$$

The no-flux conditions (3.13a) and (4.4b) hold at both orders.

In order to match the $O(1)$ solution of (4.18) on the left, we must have that

$$u_0^{\mathrm{m}}(-1, y) = 1. \tag{4.22}$$

Solving (4.20a) subject to (4.21a) and (3.13a), we obtain

$$\begin{aligned} \frac{\partial u_0^{\mathrm{m}}}{\partial y} &= 0 \\ u_0^{\mathrm{m}} &= f_0(x), \end{aligned} \tag{4.23}$$

where $f_0(x)$ is undetermined for now. However, using (4.22) and (4.4b), we can obtain boundary conditions for it:

$$f_0(-1) = 1, \qquad f_0'(0) = 0. \tag{4.24}$$

Substituting (4.23) into (4.20b) and using (3.13a) and (4.21b), we obtain

$$\begin{aligned} \frac{\partial^2 u_2^{\mathrm{m}}}{\partial y^2} &= -f_0''(x) \\ \frac{\partial u_2^{\mathrm{m}}}{\partial y} &= -f_0''(x)(y-1) && \text{(4.25a)} \\ \frac{\partial u_2^{\mathrm{m}}}{\partial y}(x, 0) &= f_0''(x) = q_u. && \text{(4.25b)} \end{aligned}$$

Solving (4.25b) subject to (4.24) and continuing to simplify, we obtain

$$\begin{aligned} f_0' &= q_u x \\ u_0^{\mathrm{m}}(x, y) = f_0 &= 1 - q_u \left(\frac{1 - x^2}{2} \right). \end{aligned} \tag{4.26a}$$

Substituting (4.25b) into (4.25a) and integrating, we have

$$u_2^{\mathrm{m}}(x, y) = q_u \left(y - \frac{y^2}{2} \right) + f_2(x), \tag{4.26b}$$

where $f_2(x)$ would be determined from the next order in the perturbation expansion. However, we wish to focus on the leading order.

Upon examination of (4.18) and (4.26a), we see that there must be a layer in the derivative (flux) in order to match the two solutions together. Because we are matching to the solution on the right, we now take $\epsilon \to 0$ in our solutions and equations for the left. Therefore, we let

$$u(x, y) = 1 + \epsilon u^{\mathrm{i}}(z, y). \tag{4.27}$$

Taking $\epsilon \to 0$ when we substitute (4.27) into (4.1), (4.6a), (3.13b), and (3.13a), we obtain, to leading order,

$$\frac{\partial^2 u^{\mathrm{i}}}{\partial z^2} + \frac{\partial^2 u^{\mathrm{i}}}{\partial y^2} = 0, \tag{4.28}$$

$$\frac{\partial u^{\mathrm{i}}}{\partial y}(z,0) = 0, \tag{4.29}$$

$$1 + \epsilon u^{\mathrm{i}}(z,1) = 1, \qquad z < 0$$

$$u^{\mathrm{i}}(z,1) = 0 \tag{4.30a}$$

$$\frac{\partial u^{\mathrm{i}}}{\partial y}(z,1) = 0, \qquad z > 0. \tag{4.30b}$$

The remaining conditions are given by matching to the outer solutions:

$$1 + \epsilon u^{\mathrm{i}}(-\infty, y) = u^{\mathrm{l}}(-1^-, y) = 1 + O(\epsilon^2)$$

$$u^{\mathrm{i}}(-\infty, y) = 0, \tag{4.31a}$$

$$\frac{\partial u^{\mathrm{i}}}{\partial z}(\infty, y) = \frac{\partial u_0^{\mathrm{m}}}{\partial x}(-1^-, y)$$

$$\frac{\partial u^{\mathrm{i}}}{\partial z}(\infty, y) = -q_u. \tag{4.31b}$$

The system (4.28)–(4.31) is essentially a potential problem in an infinite strip. The solution is more complicated to do analytically. However, this is written down mostly for completeness; the real behavior we wish to examine is in the outer regions.

Figure 4.4 shows a contour plot of u using the full equation (4.1) and the parameters in Appendix A. The solution was computed using Matlab. Note the nearly vertical contours on the right, showing that u is very nearly a function of x only. On the left, the solution is very nearly 1, with correction terms at $O(\epsilon^2)$. Since this is smaller than the size of u in the internal layer, our contours are no longer horizontal. Because our value for ϵ is 0.2, the internal layer behavior is smeared out a bit.

We note that from (4.26a) that $u_0^{\mathrm{m}}(0,y) = 1 - q_u/2$, so if $q_u > 2$, we would have a negative concentration at this order. Actually, the numerical solution in Figure 4.3 reflects a negative solution because of corrections at lower order. Essentially the problem arises because we are trying to drive a constant flux out of the system, when in actuality there may not be enough oxygen in the system to maintain the balance.

Because the equations for v are the same as those for u (with u replaced by v and q_u replaced by $-q_v$), our solutions are directly analogous:

$$v^{\mathrm{l}}(x,y) = 1 + q_v\epsilon^2(1-y), \qquad -2 \le x \le -1, \tag{4.32}$$

$$v^{\mathrm{m}}(x,y;\epsilon) = v_0^{\mathrm{m}}(x,y) + v_2^{\mathrm{m}}(x,y) + o(1), \qquad -1 \le x \le 0, \tag{4.33}$$

$$v_0^{\mathrm{m}}(x,y) = 1 + q_v\left(\frac{1-x^2}{2}\right), \tag{4.34a}$$

$$v_2^{\mathrm{m}}(x,y) = -q_v\left(y - \frac{y^2}{2}\right) + g_2(x), \tag{4.34b}$$

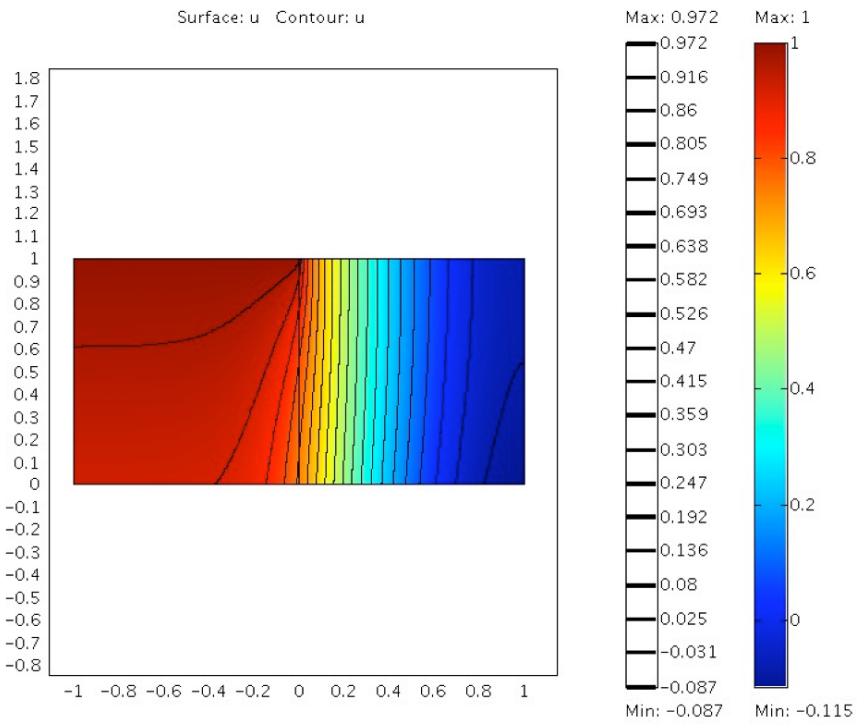

Figure 4.4. Contour plot of oxygen concentration.

$$v(x,y) = 1 + \epsilon v^{\mathrm{i}}(z,y), \tag{4.35}$$

$$\frac{\partial^2 v^{\mathrm{i}}}{\partial z^2} + \frac{\partial^2 v^{\mathrm{i}}}{\partial y^2} = 0, \tag{4.36}$$

$$\frac{\partial v^{\mathrm{i}}}{\partial y}(z,0) = 0, \tag{4.37}$$

$$v^{\mathrm{i}}(z,1) = 0, \qquad z < 0, \tag{4.38a}$$

$$\frac{\partial v^{\mathrm{i}}}{\partial y}(z,1) = 0, \qquad z > 0, \tag{4.38b}$$

$$v^{\mathrm{i}}(-\infty,y) = 0, \tag{4.39a}$$

$$\frac{\partial v^{\mathrm{i}}}{\partial z}(\infty,y) = q_v, \tag{4.39b}$$

where $g_2(x)$ would be determined from the next order in the perturbation expansion.

Figure 4.5 shows a contour plot of v using the full equation (4.2) and the parameters in Appendix A. The solution was computed using Matlab. Note that the graph is very similar to the one for u, reflecting the underlying similarity of the operators.

Now that the expressions (4.9), (4.32), and (4.34) have been calculated, we can then substitute them into (3.18) to determine the regions that are oversaturated. This was done with our numerical solutions; in particular we define the following variable:

$$S(v,T) = \frac{v - v_{\mathrm{sat}}(T)}{v_{\mathrm{sat}}(T)}. \tag{4.40}$$

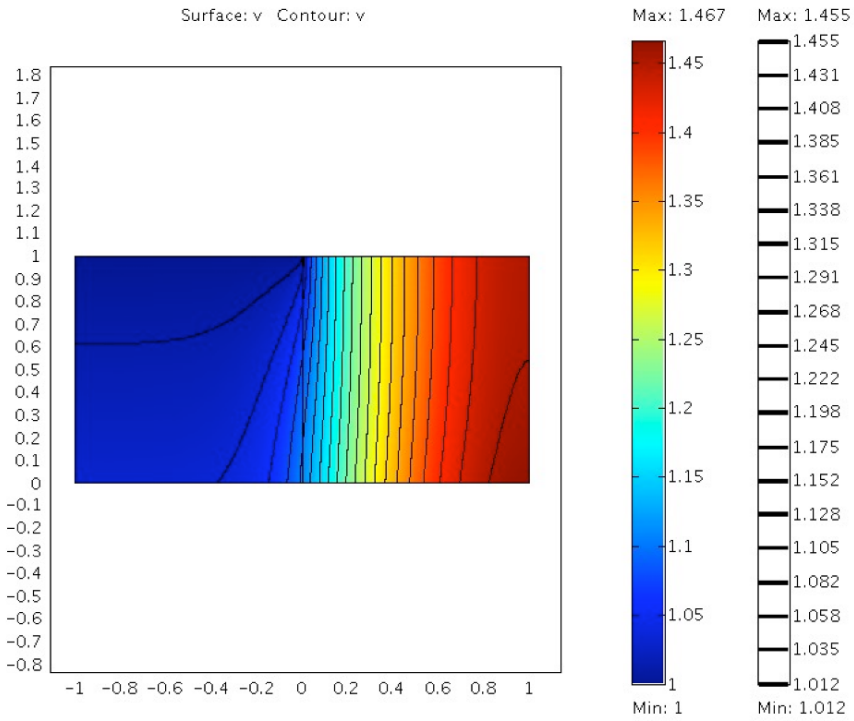

Figure 4.5. Contour plot of water vapor concentration.

Thus we see that if $S > 0$, we expect liquid water to be present and our model to break down.

Figure 4.6 shows a contour plot of S, calculated numerically in Matlab from the full equations and the parameters in Appendix A. Note that the GDL is saturated everywhere. The lowest saturation level is on the left, where the channel serves as a transport mechanism for the water. The highest saturation level is in the upper right, where the water is walled in.

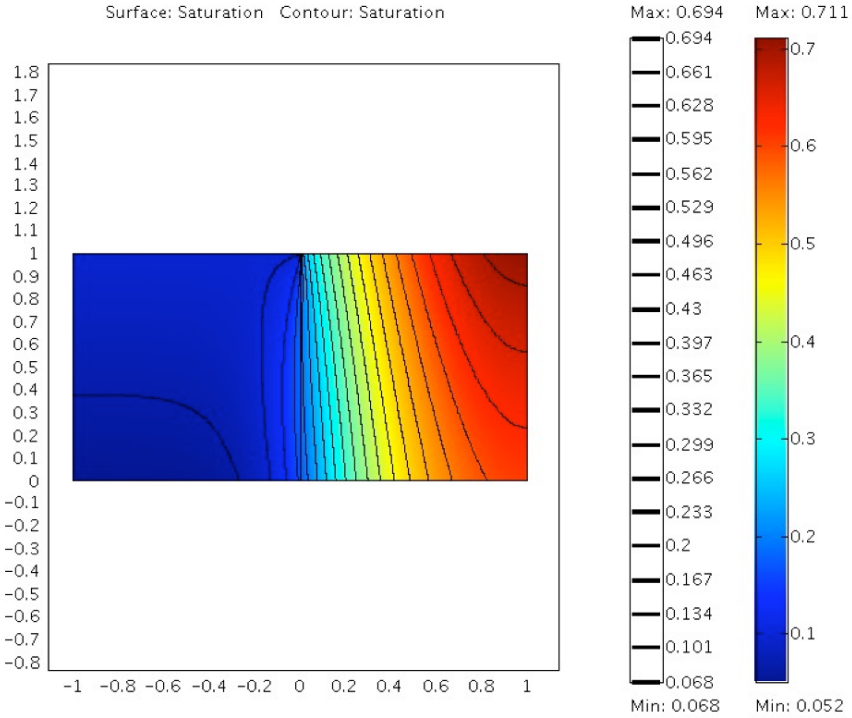

Figure 4.6. Contour plot of saturation.

Section 5: No Liquid, No Convection, Radiation Condition

As a more realistic flux condition, we note that the flux of heat, oxygen, and liquid is all driven by the reaction in the CCL. The flux is proportional to the reaction rate, which is proportional to the concentration of oxygen. Thus we have

$$\text{oxygen flux} = -D_u \frac{\partial \tilde{u}}{\partial \tilde{y}}(\tilde{x}, 0) = -\tilde{c}_u \tilde{u}(\tilde{x}, 0)$$

$$D_u \frac{\partial \tilde{u}}{\partial \tilde{y}}(\tilde{x}, 0) = \tilde{c}_u \tilde{u}(\tilde{x}, 0), \tag{5.1a}$$

where we have chosen the sign such that $\tilde{c}_u \geq 0$. In the reaction, two molecules of water are produced for every molecule of oxygen used up, so

$$D_v \frac{\partial \tilde{v}}{\partial \tilde{y}}(\tilde{x}, 0) = -2\tilde{c}_u \tilde{u}(\tilde{x}, 0). \tag{5.1b}$$

Lastly, the heat flux is given by

$$\tilde{k}_{\mathrm{C}} \frac{\partial \tilde{T}}{\partial \tilde{y}}(\tilde{x}, 0) = -\tilde{c}_T \tilde{u}(\tilde{x}, 0), \tag{5.1c}$$

where we retain the convention of keep the $\tilde{c}$s positive.

Substituting our scalings in (3.6) into (5.1), we obtain

$$D_u \frac{u_{\mathrm{l}}}{h} \frac{\partial u}{\partial y}(x, 0) = \tilde{c}_u u_{\mathrm{l}} u(x, 0)$$

$$\frac{\partial u}{\partial y}(x, 0) = c_u u(x, 0), \qquad c_u = \frac{\tilde{c}_u h}{D_u}, \tag{5.2a}$$

$$D_v \frac{v_{\mathrm{l}}}{h} \frac{\partial v}{\partial y}(x, 0) = -2\tilde{c}_u u_{\mathrm{l}} u(x, 0)$$

$$\frac{\partial v}{\partial y}(x, 0) = -c_v \epsilon^2 u(x, 0), \qquad c_v \epsilon^2 = \frac{2\tilde{c}_u u_{\mathrm{l}} h}{D_v v_{\mathrm{l}}}, \tag{5.2b}$$

$$k \frac{T_{\mathrm{l}} - T_{\mathrm{m}}}{h} \frac{\partial T}{\partial y}(x, 0) = -u_{\mathrm{l}} \tilde{c}_T u(x, 0)$$

$$\frac{\partial T}{\partial y}(x, 0) = -c_T u(x, 0), \qquad c_T = \frac{\tilde{c}_T u_{\mathrm{l}} h}{\tilde{k}_{\mathrm{C}}(T_{\mathrm{l}} - T_{\mathrm{m}})}, \tag{5.2c}$$

Here the cs are the Nusselt numbers. Again the ϵ^2 in (5.2b) has been chosen for later computational convenience, but has been motivated by Appendix A.

With (5.2a) replacing (4.6a), (4.16) is replaced by

$$\frac{\partial u_0}{\partial y}(x,0) = c_u u_0(x,0). \tag{5.3}$$

Solving (4.17) on the left subject to (3.13b) and (5.3), we have

$$\begin{aligned} u^{\mathrm{l}} &= f(x)(y-1)+1 \\ \frac{\partial u^{\mathrm{l}}}{\partial y}(x,0) = f(x) &= c_u[1-f(x)] \\ f(x) &= \frac{c_u}{1+c_u} \\ u^{\mathrm{l}}(x,y) = \frac{c_u(y-1)}{1+c_u} + 1 &= \frac{1+c_u y}{1+c_u}, \qquad -2 \le x \le -1. \end{aligned} \tag{5.4}$$

Note that the concentration always remains positive because the flux shuts off with zero concentration.

In this case, we need no perturbation series on the right. Thus we may solve (4.17) in the middle subject to (3.13a) and (5.3) to obtain

$$\begin{aligned} u^{\mathrm{m}} &= f(x) \\ \frac{\partial u^{\mathrm{m}}}{\partial y}(x,0) = 0 &= c_u f(x) \\ f(x) &= 0 \\ u^{\mathrm{m}}(x,y) &= 0, \qquad -1 \le x \le 0. \end{aligned} \tag{5.5}$$

Note that here the oxygen concentration is zero because we are not trying to force any oxygen through the GDL under the cathode, since it can't diffuse through the wall.

For later computations, it is convenient to note that

$$\frac{\partial u^{\mathrm{l}}}{\partial y}(x,0) = \frac{c_u}{1+c_u}, \tag{5.6a}$$

$$\frac{\partial u^{\mathrm{m}}}{\partial y}(x,0) = 0. \tag{5.6b}$$

The discontinuity about $x = 0$ forces an $O(1)$ internal layer, so now we let

$$u(x,y) = u^{\mathrm{i}}(z,y). \tag{5.7}$$

Substituting (5.7) into (4.1), (5.2a), (3.13a), and (3.13b), we obtain, to leading order,

$$\frac{\partial^2 u^{\mathrm{i}}}{\partial z^2} + \frac{\partial^2 u^{\mathrm{i}}}{\partial y^2} = 0, \tag{5.8}$$

$$\frac{\partial u^{\mathrm{i}}}{\partial y}(z,0) = c_u u^{\mathrm{i}}(z,0), \tag{5.9}$$

$$u^{\mathrm{i}}(z,1) = 1, \qquad z < 0 \tag{5.10a}$$

$$\frac{\partial u^{\mathrm{i}}}{\partial y}(z,1) = 0, \qquad z > 0. \tag{5.10b}$$

The remaining conditions are given by matching to the outer solutions:

$$u^{\mathrm{i}}(-\infty, y) = u^{\mathrm{l}}(-1^{-}, y) = \frac{1 + c_u y}{1 + c_u}, \tag{5.11a}$$

$$u^{\mathrm{i}}(\infty, y) = u^{\mathrm{m}}(-1^{+}, y) = 0. \tag{5.11b}$$

The system (5.8)–(5.11) is essentially a potential problem in an infinite strip. The solution is more complicated to do analytically. However, this is written down mostly for completeness; the real behavior we wish to examine is in the outer regions.

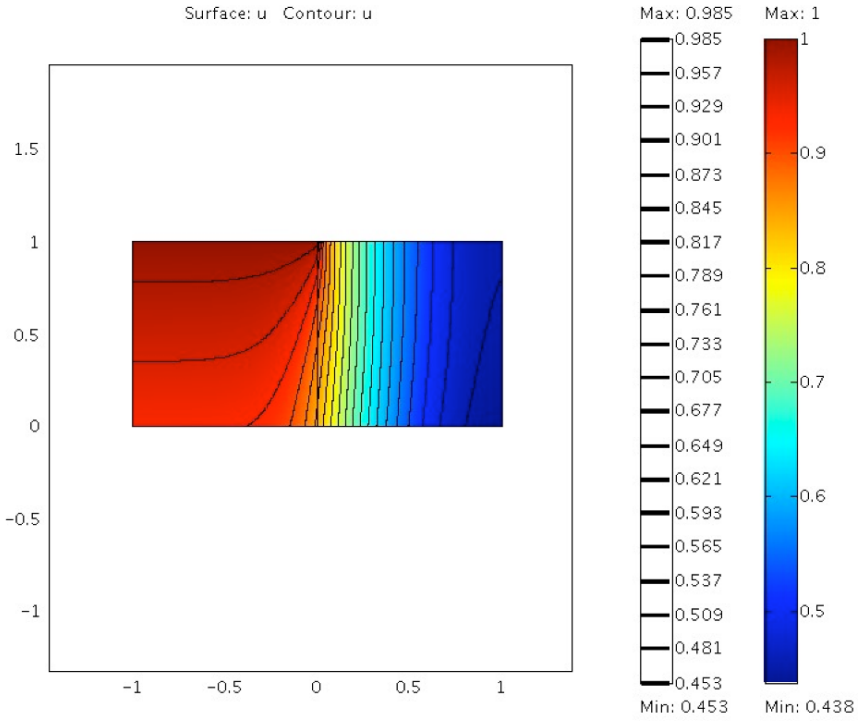

Figure 5.1. Contour plot of oxygen concentration.

Figure 5.1 shows a contour plot of u using the full equation (4.1) and the parameters in Appendix A. Note the nearly horizontal contours on the left, showing that u is very nearly a function of y only, with correction terms at $O(\epsilon^2)$. Since this is smaller than the size of u in the internal layer, our contours are no longer horizontal. Because our value for ϵ is 0.2, the internal layer behavior is smeared out a bit. Note that negative concentrations are no longer a problem.

Substituting (5.4) and (5.5) into (5.2c), we have the following conditions on T, which replace (4.6c):

$$\frac{\partial T^{\mathrm{l}}}{\partial y}(x, 0) = -\frac{c_T}{1 + c_u}, \qquad -2 \le x \le -1, \tag{5.12a}$$

$$\frac{\partial T^{\mathrm{m}}}{\partial y}(x, 0) = 0, \qquad -1 \le x \le 0. \tag{5.12b}$$

Again, we may solve the problem in strips. Since (5.12a) is of the same form as (4.6c), on the left we have that

$$T^{\mathrm{l}}(x,y) = \frac{c_T(1-y)}{1+c_u} + 1, \qquad -2 \le x \le -1. \tag{5.13a}$$

In the middle, we note that with (3.11a) and (5.12b), the solution is exactly zero:

$$T^{\mathrm{m}}(x,y) = 0, \qquad -1 \le x \le 0. \tag{5.13b}$$

Equations (5.13) replace (4.9).

The discontinuity about $x = 0$ forces an $O(1)$ internal layer, so now we let

$$T(x,y) = T^{\mathrm{i}}(z,y). \tag{5.14}$$

Substituting (5.14) into (4.3), (5.2c), (3.11a), and (3.11b), we obtain, to leading order,

$$\frac{\partial^2 T^{\mathrm{i}}}{\partial z^2} + \frac{\partial^2 T^{\mathrm{i}}}{\partial y^2} = 0, \tag{5.15}$$

$$\frac{\partial T^{\mathrm{i}}}{\partial y}(z,0) = -c_T u^{\mathrm{i}}(z,0), \tag{5.16}$$

$$T^{\mathrm{i}}(z,1) = 1, \qquad z < 0 \tag{5.17a}$$

$$T^{\mathrm{i}}(z,1) = 0, \qquad z > 0. \tag{5.17b}$$

The remaining conditions are given by matching to the outer solutions:

$$T^{\mathrm{i}}(-\infty,y) = T^{\mathrm{l}}(-1^-,y) = \frac{c_T(1-y)}{1+c_u} + 1, \tag{5.18a}$$

$$T^{\mathrm{i}}(\infty,y) = T^{\mathrm{m}}(-1^+,y) = 0. \tag{5.18b}$$

The system (5.15)–(5.18) is essentially a potential problem in an infinite strip. The solution is more complicated to do analytically. However, this is written down mostly for completeness; the real behavior we wish to examine is in the outer regions. Note that u^{i} is coupled to this problem through (5.16).

Figure 5.2 shows a contour plot of the temperature using the full equation (4.3) and the parameters in Appendix A. Note the nearly horizontal contours in the left regions, showing that the temperature is very nearly a function of y only. As expected, the temperature on the right is $O(\epsilon)$, reflecting the presence of the interior layer.

Consideration of v is slightly more complicated. Substituting (5.4) and (5.5) into (5.2b), we have the following conditions on v which replace (4.6b):

$$\frac{\partial v^{\mathrm{l}}}{\partial y}(x,0) = -\frac{c_v \epsilon^2}{1+c_u}, \qquad -2 \le x \le -1, \tag{5.19a}$$

$$\frac{\partial v^{\mathrm{m}}}{\partial y}(x,0) = 0, \qquad -1 \le x \le 0. \tag{5.19b}$$

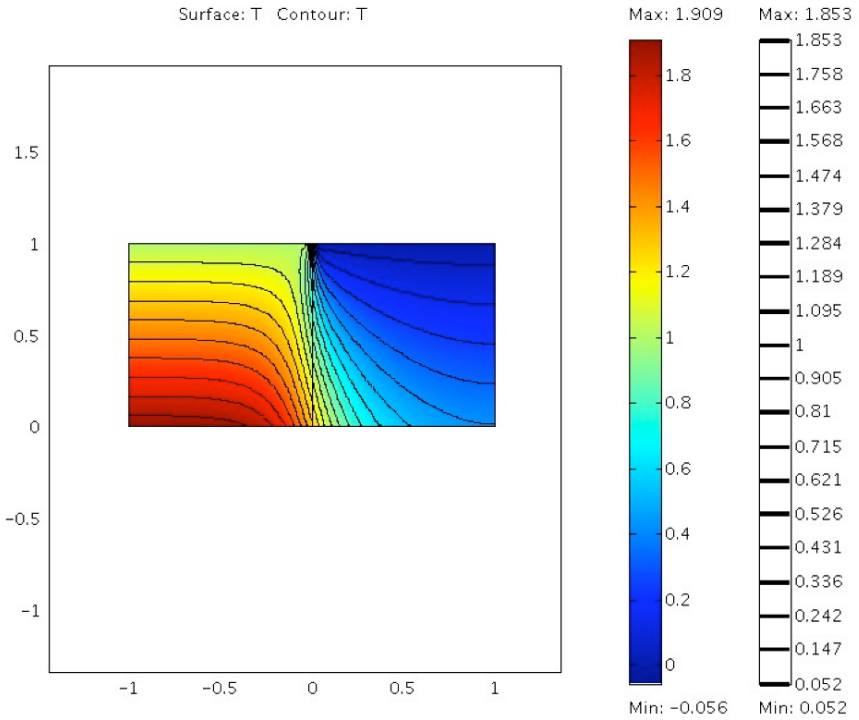

Figure 5.2. Contour plot of temperature.

But then the system for v is the same as the system for u with $-c_v\epsilon^2$ replacing c_u in the right-hand side of the boundary condition (5.6a). Thus on the left we have

$$v^{\mathrm{l}}(x,y) = \frac{-c_v\epsilon^2(y-1)}{1+c_u} + 1 = 1 + \frac{c_v\epsilon^2(1-y)}{1+c_u}, \qquad -2 \le x \le -1, \tag{5.20}$$

where we again treat the flux at leading order because it is possible for us to do so.

To obtain the leading order of v^{m}, we look at the entire domain in the limit that $\epsilon \to 0$. In that case, (5.19a) also becomes a no-flux condition. Thus we have Laplace's equation in a totally insulated box subject to (3.15b), the solution of which is $v = 1$ everywhere. This agrees with the leading order of (5.20), and it provides the leading order in the middle:

$$v_0^{\mathrm{m}}(x,y) = 1. \tag{5.21}$$

Figure 5.3 shows a contour plot of v using the full equation (4.2) and the parameters in Appendix A. Note the nearly horizontal contours on the left, showing that V is very nearly a function of y only, with correction terms at $O(\epsilon^2)$. Since this is smaller than the size of v in the internal layer, our contours are no longer horizontal. Because our value for ϵ is 0.2, the internal layer behavior is smeared out a bit. As expected, v in the entire region is within $O(\epsilon)$ of 1.

Figure 5.4 shows a contour plot of S, calculated numerically in Matlab from the full equations and the parameters in Appendix A. Note that the GDL is saturated everywhere. The form of the graph is much the same as in section 4; only the maximum of S has been reduced somewhat.

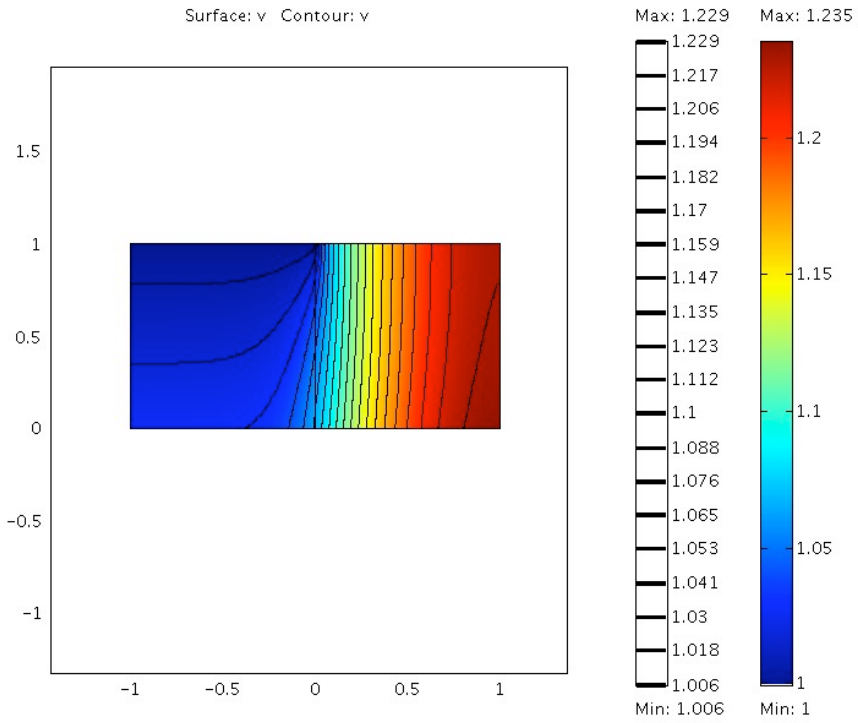

Figure 5.3. Contour plot of water vapor concentration.

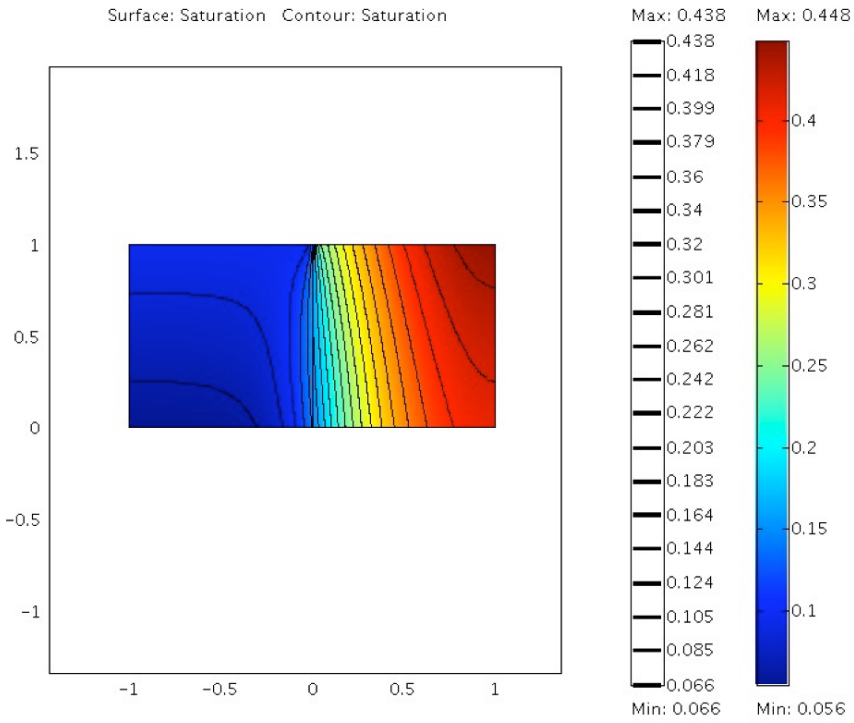

Figure 5.4. Contour plot of saturation.

Section 6: No Liquid, Convection Included

With a pressure differential included, we must now consider the entire domain $-2 \leq x \leq 2$. Substituting our scalings (3.6) into (2.14)–(2.19) and picking out the pressure terms, we have

$$\frac{\partial P^{\mathrm{m}}}{\partial y}(x,1) = 0, \qquad |x| < 1, \tag{6.1a}$$

$$\frac{P_{\mathrm{l}} - P_{\mathrm{r}}}{2} P^{\mathrm{l}}(x,1) + \frac{P_{\mathrm{l}} + P_{\mathrm{r}}}{2} = P_{\mathrm{l}}, \qquad -2 \leq x \leq -1$$

$$P^{\mathrm{l}}(x,1) = 1, \tag{6.1b}$$

$$\frac{P_{\mathrm{l}} - P_{\mathrm{r}}}{2} P^{\mathrm{r}}(x,1) + \frac{P_{\mathrm{l}} + P_{\mathrm{r}}}{2} = P_{\mathrm{r}}, \qquad 1 \leq x \leq 2$$

$$P^{\mathrm{r}}(x,1) = -1, \tag{6.1c}$$

$$\frac{\partial P^{\mathrm{l}}}{\partial x}(-2,y) = 0, \tag{6.2a}$$

$$\frac{\partial P^{\mathrm{r}}}{\partial x}(2,y) = 0, \tag{6.2b}$$

$$\frac{\partial P}{\partial y}(x,0) = 0. \tag{6.3}$$

We assume the following perturbation expansion in P:

$$P(x,y;\epsilon) = P_0(x,y) + \epsilon^2 P_2(x,y) + o(\epsilon^2). \tag{6.4}$$

Substituting (6.4) into (3.7), (6.1b), and (6.1c), we have

$$\epsilon^2 \frac{\partial^2 (P_0 + P_2)}{\partial x^2} + \frac{\partial^2 (P_0 + P_2)}{\partial y^2} = 0$$

$$\frac{\partial^2 P_0}{\partial y^2} = 0, \tag{6.5a}$$

$$\frac{\partial^2 P_2}{\partial y^2} = -\frac{\partial^2 P_0}{\partial x^2}, \tag{6.5b}$$

$$P_0^{\mathrm{l}}(x,1) = 1, \tag{6.6a}$$

$$P_0^{\mathrm{r}}(x,1) = -1. \tag{6.6b}$$

The remaining no-flux conditions on the pressure [(6.1a), (6.2), and (6.3)] hold for both orders, so we do not write them down here.

On the left, we may solve (6.5a) subject to (6.3) and (6.6a) to yield

$$\frac{\partial P_0^{\mathrm{l}}}{\partial y} = 0$$

$$P_0^{\mathrm{l}}(x,y) = 1. \tag{6.7a}$$

Substituting (6.7a) into (6.5b) and integrating subject to (6.3), we have

$$\begin{aligned} \frac{\partial^2 P_2^{\mathrm{l}}}{\partial y^2} &= 0 \\ \frac{\partial P_2^{\mathrm{l}}}{\partial y} &= 0. \end{aligned} \tag{6.7b}$$

Similarly, on the right we may solve (6.5a) subject to (6.3) and (6.6b) to yield

$$P_0^{\mathrm{r}}(x,y) = -1, \tag{6.8a}$$

$$\frac{\partial P_2^{\mathrm{r}}}{\partial y} = 0. \tag{6.8b}$$

Since we must match P_0^{m} to the solutions on left and right, (6.7a) and (6.8a) provide the following new boundary conditions on the middle problem:

$$P_0^{\mathrm{m}}(-1,y) = 1, \qquad P_0^{\mathrm{m}}(1,y) = -1. \tag{6.9}$$

In the middle, we may solve (6.5a) subject to (6.1a) and (6.3) to yield

$$\frac{\partial P_0^{\mathrm{m}}}{\partial y} = 0 \tag{6.10}$$

$$P_0^{\mathrm{m}}(x,y) = f_0(x), \tag{6.11a}$$

$$f_0(-1) = 1, \quad f_0(1) = -1, \tag{6.11b}$$

where the boundary conditions come from (6.9).

Substituting (6.11a) into (6.5b) and using (6.1a) and (6.3), we obtain

$$\begin{aligned} \frac{\partial^2 P_2^{\mathrm{m}}}{\partial y^2} &= -f_0''(x) \\ \frac{\partial P_2^{\mathrm{m}}}{\partial y} &= -f_0''(x)(y-1) \end{aligned} \tag{6.12a}$$

$$\frac{\partial P_2^{\mathrm{m}}}{\partial y}(x,0) = f_0''(x) = 0. \tag{6.12b}$$

Solving (6.12b) subject to (6.11b) and continuing to simplify, we obtain

$$\begin{aligned} f_0 &= Ax + B \\ -A + B &= 1 \\ A + B &= -1 \\ f_0 &= -x \\ P_0^{\mathrm{m}}(x,y) &= -x. \end{aligned} \tag{6.13a}$$

Integrating (6.12a), we have

$$P_2^{\mathrm{m}}(x,y) = f_2(x), \tag{6.13b}$$

where $f_2(x)$ would be determined from the next order in the perturbation expansion.

Upon examination of (6.7a) and (6.13a), we see that there must be a layer in the derivative in order to match the two solutions together. Therefore, we let

$$P(x,y) = 1 + \epsilon P^{\mathrm{i}}(z,y). \tag{6.14}$$

When we substitute (6.14) into (3.7), (6.3), (6.1b), and (6.1a), we obtain, to leading order,

$$\frac{\partial^2 P^{\mathrm{i}}}{\partial z^2} + \frac{\partial^2 P^{\mathrm{i}}}{\partial y^2} = 0, \tag{6.15}$$

$$\frac{\partial P^{\mathrm{i}}}{\partial y}(z,0) = 0, \tag{6.16}$$

$$1 + \epsilon P^{\mathrm{i}}(z,1) = 1, \qquad z < 0$$

$$P^{\mathrm{i}}(z,1) = 0 \tag{6.17a}$$

$$\frac{\partial P^{\mathrm{i}}}{\partial y}(z,1) = 0, \qquad z > 0. \tag{6.17b}$$

The remaining conditions are given by matching to the outer solutions:

$$1 + \epsilon P^{\mathrm{i}}(-\infty,y) = P^{\mathrm{l}}(-1^-,y) = 1$$

$$P^{\mathrm{i}}(-\infty,y) = 0, \tag{6.18a}$$

$$\frac{\partial P^{\mathrm{i}}}{\partial z}(\infty,y) = \frac{\partial P_0^{\mathrm{m}}}{\partial x}(-1^-,y)$$

$$\frac{\partial P^{\mathrm{i}}}{\partial z}(\infty,y) = -1. \tag{6.18b}$$

The system (6.15)–(6.18) is essentially a potential problem in an infinite strip. The solution is more complicated to do analytically. However, this is written down mostly for completeness; the real behavior we wish to examine is in the outer regions. For this reason, we do not write down all the equations for the similar internal layer that would be necessary about $x = 1$, $P = -1$.

Now we couple the pressure results back into the u and v equations. As a practical matter, the temperature equations would be unaffected, since we calculate those solutions to leading order and don't concern ourselves with the next-order correction.

For u and v, if we use the boundary conditions in section 5, we would also not see a large effect, since in that case we only compute leading order solutions in the left and middle. On the right there would be some effect because (3.13c) and (3.15c) require tracking to $O(\epsilon^2)$. If we were to use the conditions in section 4, then the consistency equations such as (4.20b) and (4.25b) would change. But as shown in section 4, those boundary conditions in section 4 can lead to negative conentrations in certain situations. Therefore, further work should proceed with the boundary conditions in section 5.

Section 7: Two-Component Gas Diffusion: Derivation

We now wish to consider the effects of more complicated diffusive processes on our model. Here we follow some of the basic descriptions in [5]. First, we assume that the permeability of the GDL to gases is now given by

$$\kappa_{\mathrm{g}}(1-W)^3, \tag{7.1}$$

where the value of κ_{g} used is the same one as in previous sections where the permeability was assumed constant. For our purposes we will take W to be a constant.

Second, we replace standard Fickian diffusion in equation (2.4) for the oxygen with the following:

$$\nabla \cdot \left(D_u \tilde{G} \nabla \left(\frac{\tilde{u}}{\tilde{G}} \right) - \tilde{u} \tilde{\mathbf{V}}_{\mathrm{g}} \right) = 0, \tag{7.2}$$

where $\tilde{G}$ is the molar density of all the gases together. In reality, the three main species are oxygen, water vapor, and nitrogen. For the purposes of this section, however, the nitrogen is irrelevant, so without loss of generality we may take

$$\tilde{G} = \tilde{u} + \tilde{v}. \tag{7.3}$$

We may simplify (7.2) by inserting (2.11) and the ideal gas law to obtain

$$\nabla \cdot \left(D_u \tilde{G} \nabla \left(\frac{\tilde{u}}{\tilde{G}} \right) - \tilde{u} \left(-\frac{\kappa_{\mathrm{g}}(\theta)}{\mu} \nabla \tilde{P} \right) \right) = 0$$

$$\nabla \cdot \left(D_u \tilde{G} \nabla \left(\frac{\tilde{u}}{\tilde{G}} \right) + \frac{\kappa_{\mathrm{g}}(\theta)}{\mu} \tilde{u} \nabla (\tilde{G} R T) \right) = 0.$$

If we moreover assume that the system is isothermal, we may pull the temperature out of the gradient to obtain

$$\nabla \cdot \left(D_u \tilde{G} \nabla \left(\frac{\tilde{u}}{\tilde{G}} \right) + \frac{\kappa_{\mathrm{g}}(\theta) R T}{\mu} \tilde{u} \nabla \tilde{G} \right) = 0. \tag{7.4a}$$

For the water vapor $\tilde{v}$, we have a similar equation once we ignore evaporation and condensation:

$$\nabla \cdot \left(D_v \tilde{G} \nabla \left(\frac{\tilde{v}}{\tilde{G}} \right) + \frac{\kappa_{\mathrm{g}}(\theta) R T}{\mu} \tilde{v} \nabla \tilde{G} \right) = 0. \tag{7.4b}$$

If we moreover assume that $D_u = D_v = D$, then we may sum (7.4) to yield

$$\nabla \cdot \left(D \tilde{G} \nabla \left(\frac{\tilde{u} + \tilde{v}}{\tilde{G}} \right) + \frac{\kappa_{\mathrm{g}}(\theta) R T}{\mu} (\tilde{u} + \tilde{v}) \nabla \tilde{G} \right) = 0$$

$$\frac{1}{2} \nabla \cdot \left(\tilde{G} \nabla \tilde{G} \right) = \frac{1}{2} \nabla^2 (\tilde{G}^2) = 0$$

$$\frac{\partial^2 \tilde{G}^2}{\partial \tilde{x}^2} + \frac{\partial^2 \tilde{G}^2}{\partial \tilde{y}^2} = 0. \tag{7.5}$$

Next we wish to write (7.4a) in more detail. We begin by defining the new variable

$$r = \frac{\tilde{u}}{\tilde{G}\Phi_u}, \tag{7.6}$$

where Φ_u is the volume fraction of oxygen. (Note that with this convention, θ should really be denoted as Φ_θ. However, we use θ to agree with the literature.)

The motivation for the scaling is as follows. In the left channel, the value of $\tilde{G}$ is given by the characteristic value G_l:

$$\tilde{G}(\tilde{x}, h) = G_\mathrm{l}, \quad -2d \le \tilde{x} \le d, \tag{7.7a}$$

and the concentration of oxygen is then given by

$$\tilde{u}(\tilde{x}, h) = u_\mathrm{l} = \Phi_\mathrm{u} G_\mathrm{l}, \quad -2d \le \tilde{x} \le d, \tag{7.7b}$$

Combining (7.7) to form a boundary condition for the dimensionless variable r, we have that

$$r^\mathrm{l}(x, 1) = 1, \quad -2 \le x \le -1. \tag{7.8}$$

Substituting (7.6) into (7.4a), we obtain

$$\begin{aligned}
\nabla \cdot \left(D\tilde{G}\nabla(\Phi_\mathrm{u} r) + \frac{\kappa_\mathrm{g}(\theta)RT}{\mu}(\tilde{G}\Phi_u r)\nabla(\tilde{G}) \right) &= 0 \\
\nabla \cdot \left(D\tilde{G}\nabla r + \frac{\kappa_\mathrm{g}(\theta)RT}{2\mu} r \nabla(\tilde{G}^2) \right) &= 0 \\
D\left[\frac{\partial}{\partial \tilde{x}} \left(\tilde{G}\frac{\partial r}{\partial \tilde{x}} \right) + \frac{\partial}{\partial \tilde{y}} \left(\tilde{G}\frac{\partial r}{\partial \tilde{y}} \right) \right] + \frac{\kappa_\mathrm{g}(\theta)RT}{2\mu} \left[\frac{\partial}{\partial \tilde{x}} \left(r\frac{\partial \tilde{G}^2}{\partial \tilde{x}} \right) + \frac{\partial}{\partial \tilde{y}} \left(r\frac{\partial \tilde{G}^2}{\partial \tilde{y}} \right) \right] &= 0.
\end{aligned} \tag{7.9}$$

To scale (7.5) and (7.9), we let

$$s(x, y) = \frac{\tilde{G}^2(\tilde{x}, \tilde{y})}{G_\mathrm{l}^2}. \tag{7.10}$$

Substituting our scalings in (3.6a) and (7.10) into (7.5) and (7.9), we obtain

$$\begin{aligned}
\frac{G_\mathrm{l}^2}{d^2}\frac{\partial^2 s}{\partial x^2} + \frac{G_\mathrm{l}^2}{h^2}\frac{\partial^2 s}{\partial y^2} &= 0 \\
\epsilon^2 \frac{\partial^2 s}{\partial x^2} + \frac{\partial^2 s}{\partial y^2} &= 0,
\end{aligned} \tag{7.11a}$$

$$\begin{aligned}
D\left[\frac{G_\mathrm{l}}{d^2}\frac{\partial}{\partial x}\left(\sqrt{s}\frac{\partial r}{\partial x} \right) + \frac{G_\mathrm{l}}{h^2}\frac{\partial}{\partial y}\left(\sqrt{s}\frac{\partial r}{\partial y} \right) \right] & \\
+ \frac{\kappa_\mathrm{g}(\theta)RT}{2\mu} \left[\frac{G_\mathrm{l}^2}{d^2}\frac{\partial}{\partial x}\left(r\frac{\partial s}{\partial x} \right) + \frac{G_\mathrm{l}^2}{h^2}\frac{\partial}{\partial y}\left(r\frac{\partial s}{\partial y} \right) \right] &= 0
\end{aligned}$$

$$\mathrm{Pe}_G^{-1}\left[\epsilon^2\frac{\partial}{\partial x}\left(\sqrt{s}\frac{\partial r}{\partial x}\right)+\frac{\partial}{\partial y}\left(\sqrt{s}\frac{\partial r}{\partial y}\right)\right]+\frac{1}{2}\left[\epsilon^2\frac{\partial}{\partial x}\left(r\frac{\partial s}{\partial x}\right)+\frac{\partial}{\partial y}\left(r\frac{\partial s}{\partial y}\right)\right]=0, \quad (7.11b)$$

$$\mathrm{Pe}_G=\frac{\kappa_{\mathrm{g}}(\theta)RTG_{\mathrm{l}}}{D\mu}. \quad (7.12)$$

Here we use the subscript G to note that the Péclet number here is based on the total gas concentration, not one species. This definition of Pe_G agrees with the definition of R_g in [13].

For boundary conditions, we note that without an imposed pressure gradient, we are in the geometry of Figure 4.1. Thus symmetry forces the following conditions, analogous to (3.14a) and (4.4):

$$\frac{\partial r^{\mathrm{l}}}{\partial x}(-2,y)=0, \quad (7.13a)$$

$$\frac{\partial s^{\mathrm{l}}}{\partial x}(-2,y)=0, \quad (7.13b)$$

$$\frac{\partial r^{\mathrm{m}}}{\partial x}(0,y)=0, \quad (7.14a)$$

$$\frac{\partial s^{\mathrm{m}}}{\partial x}(0,y)=0. \quad (7.14b)$$

Similarly, the conditions at the wall are also similar to (3.13a):

$$\frac{\partial r^{\mathrm{m}}}{\partial y}(x,1)=0, \qquad -1<x<0, \quad (7.15a)$$

$$\frac{\partial s^{\mathrm{m}}}{\partial y}(x,1)=0, \qquad -1<x<0. \quad (7.15b)$$

At the exposed channel, from (7.7a) we have that

$$s^{\mathrm{l}}(x,1)=1, \quad -2\le x\le -1. \quad (7.16)$$

To obtain the conditions at the reacting surface, we use the reasoning behind the derivation of (5.1), namely that the flux should be proportional to the reaction rate, which is proportional to the concentration of oxygen. However, the fluxes are now given by the expression in (7.4), so the boundary conditions on u and v become

$$\left[D\tilde{G}\frac{\partial}{\partial\tilde{y}}\left(\frac{\tilde{u}}{\tilde{G}}\right)+\frac{\kappa_{\mathrm{g}}(\theta)RT}{\mu}\tilde{u}\frac{\partial\tilde{G}}{\partial\tilde{y}}\right](\tilde{x},0)=\tilde{c}_u\tilde{u}(\tilde{x},0), \quad (7.17a)$$

$$\left[D\tilde{G}\frac{\partial}{\partial\tilde{y}}\left(\frac{\tilde{v}}{\tilde{G}}\right)+\frac{\kappa_{\mathrm{g}}(\theta)RT}{\mu}\tilde{v}\frac{\partial\tilde{G}}{\partial\tilde{y}}\right](\tilde{x},0)=-2\tilde{c}_u\tilde{u}(\tilde{x},0). \quad (7.17b)$$

Note that since the membrane is permeable, the velocity there is nonzero. Summing (7.17), we obtain the same type of cancellation for the diffusive flux as in (7.5):

$$\frac{\kappa_{\mathrm{g}}(\theta)RT}{\mu}\left(\tilde{G}\frac{\partial\tilde{G}}{\partial\tilde{y}}\right)(\tilde{x},0) = -\tilde{c}_u(r\Phi_u\tilde{G})(\tilde{x},0)$$
$$\frac{G_{\mathrm{l}}}{h}\frac{\partial\sqrt{s}}{\partial y}(x,0) = -\frac{\tilde{c}_u\mu}{\kappa_{\mathrm{g}}(\theta)RT}\Phi_u r(x,0)$$
$$\frac{\partial\sqrt{s}}{\partial y}(x,0) = -\frac{\tilde{c}_u h}{D}\frac{D\mu}{\kappa_{\mathrm{g}}(\theta)RTG_{\mathrm{l}}}\Phi_u r(x,0) = -\frac{c_u}{\mathrm{Pe}_G}\Phi_u r(x,0), \quad (7.18a)$$

where we have used (5.2a) and (7.12). Rewriting (7.17a) in terms of r, we have

$$\left[\frac{D}{h}\tilde{G}\frac{\partial(\Phi_u r)}{\partial y} + \frac{\kappa_{\mathrm{g}}(\theta)RT}{\mu h}(\Phi_u\tilde{G}r)\frac{\partial\tilde{G}}{\partial\tilde{y}}\right](\tilde{x},0) = \tilde{c}_u(\Phi_u\tilde{G}r)(\tilde{x},0),$$
$$\left[\frac{\partial r}{\partial y} + \frac{\kappa_{\mathrm{g}}(\theta)RTG_{\mathrm{l}}}{\mu D}r\frac{\partial\sqrt{s}}{\partial\tilde{y}}\right](x,0) = \frac{\tilde{c}_u h}{D}r(x,0),$$
$$\left[\frac{\partial r}{\partial y} + \mathrm{Pe}_G r\left(-\frac{c_u\Phi_u}{\mathrm{Pe}_G}r\right)\right](x,0) = c_u r(x,0),$$
$$\frac{\partial r}{\partial y}(x,0) = c_u(r+\Phi_u r^2)(x,0), \quad (7.18b)$$

where we have used (7.18a).

In order to simplify the analysis that follows, we introduce the additional parameter

$$m = \frac{c_u\Phi_u}{\mathrm{Pe}_G} \quad (7.19)$$

into (7.18), yielding

$$\frac{\partial\sqrt{s}}{\partial y}(x,0) = -mr(x,0), \quad (7.20a)$$
$$\frac{1}{\mathrm{Pe}_G}\frac{\partial r}{\partial y}(x,0) = \frac{c_u\Phi_u}{\mathrm{Pe}_G}\left(\frac{r}{\Phi_u}+r^2\right)(x,0) = m\left(\frac{r}{\Phi_u}+r^2\right)(x,0). \quad (7.20b)$$

Section 8: Two-Component Gas Diffusion: Asymptotic Solution

One-dimensional case. We begin by considering the one dimensional (1D) case ($\epsilon = 0$). In this case, we ignore the conditions at the wall and instead focus on the channel. Thus we substitute this assumption into (7.11), (7.16), (7.20), and (7.8) to obtain

$$\frac{d^2 s}{dy^2} = 0, \tag{8.1}$$

$$s(1) = 1, \tag{8.2a}$$

$$\frac{d\sqrt{s}}{dy}(0) = -mr(0), \tag{8.2b}$$

$$\mathrm{Pe}_G^{-1} \frac{d}{dy}\left(\sqrt{s}\frac{dr}{dy}\right) + \frac{1}{2}\frac{d}{dy}\left(r\frac{ds}{dy}\right) = 0, \tag{8.3}$$

$$r(1) = 1, \tag{8.4a}$$

$$\frac{1}{\mathrm{Pe}_G}\frac{dr}{dy}(0) = m\left(\frac{r}{\Phi_u} + r^2\right)(0). \tag{8.4b}$$

Asymptotic solution. Though an exact solution for the one-dimensional case is derived later in this section, we wish to solve the problem asymptotically to illustrate how the procedure might be used for a more complicated two-dimensional problem.

Since on the cathode side, $\mathrm{Pe}_G^{-1} \ll 1$, we expand the solution with respect to Pe_G^{-1} as

$$s(x;\mathrm{Pe}_G) = s_0(x) + \mathrm{Pe}_G^{-1} s_1(x) + \cdots, \qquad r(x;\mathrm{Pe}_G) = r_0(x) + \mathrm{Pe}_G^{-1} r_1(x) + \cdots. \tag{8.5}$$

The algebra will proceed more smoothly if we recall the following result:

$$\sqrt{s_0 + \mathrm{Pe}_G^{-1} s_1} = \sqrt{s_0}\sqrt{1 + \frac{\mathrm{Pe}_G^{-1} s_1}{s_0}} = \sqrt{s_0} + \frac{\mathrm{Pe}_G^{-1} s_1}{2\sqrt{s_0}} + \cdots. \tag{8.6}$$

We wish to obtain the leading order solution for both r and s. As shown below, that will necessitate keeping additional terms in the s equations. Thus we substitute (8.5) into (8.1)–(8.4), keeping the necessary orders:

$$\frac{d^2 s_0}{dy^2} = 0, \tag{8.7a}$$

$$\frac{d^2 s_1}{dy^2} = 0, \tag{8.7b}$$

$$s_0(1) = 1, \tag{8.8a}$$

$$s_1(1) = 0, \tag{8.8b}$$

$$\frac{d}{dy}\left(\sqrt{s_0} + \frac{\mathrm{Pe}_G^{-1} s_1}{2\sqrt{s_0}}\right)(0) = -m(r_0 + \mathrm{Pe}_G^{-1} r_1)(0)$$

$$\frac{d\sqrt{s_0}}{dy}(0) = -m r_0(0) \tag{8.9a}$$

$$\frac{d}{dy}\left(\frac{s_1}{2\sqrt{s_0}}\right)(0) = -m r_1(0), \tag{8.9b}$$

$$\mathrm{Pe}_G^{-1}\frac{d}{dy}\left(\sqrt{s_0}\frac{dr_0}{dy}\right) + \frac{1}{2}\frac{d}{dy}\left(r_0\frac{ds_0}{dy} + \mathrm{Pe}_G^{-1}\left(r_0\frac{ds_1}{dy} + r_1\frac{ds_0}{dy}\right)\right) = 0$$

$$\frac{1}{2}\frac{d}{dy}\left(r_0\frac{ds_0}{dy}\right) = 0, \tag{8.10a}$$

$$\frac{d}{dy}\left(\sqrt{s_0}\frac{dr_0}{dy} + \frac{1}{2}\left(r_0\frac{ds_1}{dy} + r_1\frac{ds_0}{dy}\right)\right) = 0, \tag{8.10b}$$

$$r_0(1) = 1, \tag{8.11}$$

$$\frac{1}{\mathrm{Pe}_G}\frac{d(r_0 + \mathrm{Pe}_G^{-1} r_1)}{dy}(0) = m\left[\frac{r_0 + \mathrm{Pe}_G^{-1} r_1}{\Phi_u} + (r_0 + \mathrm{Pe}_G^{-1} r_1)^2\right](0)$$

$$m r_0\left(\frac{1}{\Phi_u} + r_0\right)(0) = 0, \tag{8.12a}$$

$$m\left(\frac{r_1}{\Phi_u} + 2 r_0 r_1\right)(0) = \frac{dr_0}{dy}(0). \tag{8.12b}$$

(Note that in (8.11) we have kept only the leading-order term, since it is the only ones needed for the analysis.)

If we recall that r_0 cannot be negative on physical grounds, (8.12a) reduces to

$$r_0(0) = 0, \tag{8.13}$$

in which case (8.9a) becomes

$$\frac{d\sqrt{s_0}}{dy}(0) = 0. \tag{8.14}$$

Solving (8.7a) subject to (8.8a) and (8.14), we obtain

$$s_0 = 1. \tag{8.15}$$

If we substitute (8.15) into (8.10a), we see that it is automatically satisfied, so the determination of r_0 must wait until the next order.

Substituting (8.13) and (8.15) into (8.10b), (8.9b), and (8.12b), we obtain

$$\frac{d^2 r_0}{dy^2} + \frac{1}{2}\frac{d}{dy}\left(r_0\frac{ds_1}{dy}\right) = 0, \tag{8.16}$$

$$\frac{1}{2}\frac{ds_1}{dy}(0) = -m r_1(0), \tag{8.17a}$$

$$\frac{m}{\Phi_u} r_1(0) = \frac{dr_0}{dy}(0). \tag{8.17b}$$

Combining (8.17), we have

$$\frac{1}{2}\frac{ds_1}{dy}(0) = -\Phi_{\mathrm{u}}\frac{dr_0}{dy}(0). \tag{8.18}$$

Solving (8.7b) subject to (8.8b) and (8.18), we obtain

$$s_1 = -2\Phi_{\mathrm{u}}\frac{dr_0}{dy}(0)(y-1). \tag{8.19}$$

Substituting (8.19) into (8.16) and solving subject to (8.13), we have

$$\begin{aligned}
\frac{d^2 r_0}{dy^2} - \Phi_{\mathrm{u}}\frac{dr_0}{dy}(0)\frac{dr_0}{dy} &= 0 \\
\frac{dr_0}{dy} - \Phi_{\mathrm{u}}\frac{dr_0}{dy}(0) r_0 &= \frac{dr_0}{dy}(0), \\
r_0 &= \frac{1}{\Phi_u}\left[\exp\left(\Phi_u\frac{dr_0}{dy}(0)y\right) - 1\right].
\end{aligned}$$

Then substituting $y = 1$ into the above and using (8.11), the full expressions can be obtained:

$$\begin{aligned}
r_0(1) = 1 &= \frac{1}{\Phi_u}\left[\exp\left(\Phi_u\frac{dr_0}{dy}(0)\right) - 1\right]. \\
\log(1+\Phi_u) &= \Phi_u\frac{dr_0}{dy}(0) \\
r_0(y) &= \frac{(1+\Phi_u)^y - 1}{\Phi_u}, \qquad (8.20\mathrm{a}) \\
s_1(y) &= 2\log(1+\Phi_u)(1-y). \qquad (8.20\mathrm{b})
\end{aligned}$$

Thus the asymptotic solution to these orders is

$$\begin{aligned}
r(y) &= \frac{(1+\Phi_u)^y - 1}{\Phi_u} + O(\mathrm{Pe}_G^{-1}), \qquad (8.21\mathrm{a}) \\
s(y) &= 1 + 2\log(1+\Phi_u)(1-y)\mathrm{Pe}_G^{-1} + O(\mathrm{Pe}_G^{-2}). \qquad (8.21\mathrm{b})
\end{aligned}$$

It is interesting to note that the zeroth order solution for the relative concentration of the reactant r (oxygen) is not a constant.

Comparison to the exact solution. For the one-dimensional case, we may solve the problem exactly as follows. Solving (8.1) subject to (8.2a), we have

$$s = 1 + 2A_s(y-1), \tag{8.22}$$

where A_s is an undetermined constant. Substituting (8.22) into (8.3) and integrating, we have

$$\begin{aligned}
\mathrm{Pe}_G^{-1}\left(\sqrt{s}\frac{dr}{dy}\right) + A_s r &= A_r \\
\mathrm{Pe}_G^{-1}\frac{dr}{dy} + r\frac{A_s}{\sqrt{s}} &= \frac{A_r}{A_s}\frac{A_s}{\sqrt{s}}.
\end{aligned} \tag{8.23}$$

Upon noting that

$$\frac{d(\sqrt{s})}{dy} = \frac{1}{2\sqrt{s}}\frac{ds}{dy} = \frac{A_s}{\sqrt{s}}, \tag{8.24}$$

we may evaluate (8.23) at $y = 0$ to obtain

$$\begin{aligned} \mathrm{Pe}_G^{-1}\frac{dr}{dy}(0) + \left(r\frac{d(\sqrt{s})}{dy}\right)(0) &= \frac{A_r}{A_s}\frac{d(\sqrt{s})}{dy}(0) \\ m\left(\frac{r}{\Phi_u} + r^2\right)(0) - mr^2(0) &= \frac{A_r}{A_s}(-mr)(0) \\ \frac{A_r}{A_s} &= -\frac{1}{\Phi_u}, \end{aligned} \tag{8.25}$$

where we have used (8.2b) and (8.4b).

Substituting (8.24) and (8.25) into (8.23) and integrating, we have

$$\begin{aligned} \frac{d}{dy}\left(r\exp\left(\mathrm{Pe}_G\sqrt{s}\right)\right) &= -\frac{1}{\Phi_u}\frac{A_s\mathrm{Pe}_G}{\sqrt{s}}\exp\left(\mathrm{Pe}_G\sqrt{s}\right) \\ r &= -\frac{1}{\Phi_u} + \left(1 + \frac{1}{\Phi_u}\right)\exp\left(\mathrm{Pe}_G(1-\sqrt{s})\right), \end{aligned} \tag{8.26}$$

where we have used (8.2a) and (8.4a). To solve for s, it is more convenient to consider the quantity

$$s(0) = 1 - 2A_s, \tag{8.27a}$$

thus writing (8.22) as

$$s(y) = 1 + [1 - s(0)](y - 1). \tag{8.27b}$$

Substituting (8.26) and (8.27b) into (8.2b), we have

$$\begin{aligned} \frac{d\sqrt{s}}{dy}(0) = \frac{1-s(0)}{2\sqrt{s(0)}} = -mr(0) &= \frac{m}{\Phi_u} - m\left(1 + \frac{1}{\Phi_u}\right)\exp\left(\mathrm{Pe}_G(1-\sqrt{s(0)}\right) \\ \frac{s(0)-1}{2m\sqrt{s(0)}} &= -\frac{1}{\Phi_u} + \left(1 + \frac{1}{\Phi_u}\right)\exp\left(\mathrm{Pe}_G(1-\sqrt{s(0)}\right). \end{aligned} \tag{8.28}$$

To check with our asymptotic results, we examine (8.28) for large Pe_G. If $s(0) < 1$, the left-hand side is negative while the right hand side is large and positive. If $s(0) > 1$, the left-hand side is positive while the right-hand side is negative. Thus we must have that

$$s(0) = 1 + 2\mathrm{Pe}_G^{-1}B + \cdots. \tag{8.29}$$

Substituting (8.29) into (8.28), we have, to leading order,

$$\frac{\mathrm{Pe}_G^{-1}B}{m} = -\frac{1}{\Phi_u} + \left(1 + \frac{1}{\Phi_u}\right)\exp\left(\mathrm{Pe}_G(1-(1+\mathrm{Pe}_G^{-1}B)\right)$$

$$
\begin{aligned}
1 &= (\Phi_u + 1)e^{-B} \\
B &= \log(\Phi_u + 1) \\
s(y) &\sim 1 + [1 - (1 + 2\mathrm{Pe}_G^{-1} B)](y-1) = 1 + 2\mathrm{Pe}_G^{-1} \log(\Phi_u + 1)(1-y), \qquad (8.30a) \\
r(y) &= -\frac{1}{\Phi_u} + \left(1 + \frac{1}{\Phi_u}\right) \exp\left(\mathrm{Pe}_G(1 - \sqrt{1 + 2\mathrm{Pe}_G^{-1} \log(\Phi_u + 1)(1-y)})\right) \\
&= \frac{1}{\Phi_u}\left[-1 + (\Phi_u + 1)\exp\left(-\log(\Phi_u + 1)(1-y)\right)\right] \\
&= \frac{(\Phi_u + 1)^{y-1+1} - 1}{\Phi_u} = \frac{(\Phi_u + 1)^y - 1}{\Phi_u}. \qquad (8.30b)
\end{aligned}
$$

Note that (8.30) agree with (8.21).

Two Dimensional Case. We could look for asymptotic solutions of the 2D case by expand the solutions in Pe_G^{-1} as in the 1D case:

$$
s(x,y) = s_0 + \mathrm{Pe}_G^{-1} s_1 + \cdots, \qquad r(x,y) = r_0 + \mathrm{Pe}_G^{-1} r_1 + \cdots. \qquad (8.31a)
$$

However, if we are interested only in the leading order behavior, we can use a "quick and dirty" transformation motivated by (8.21b):

$$
s(x,y) = 1 + \mathrm{Pe}_G^{-1} s_1. \qquad (8.31b)
$$

Substituting (8.31) into (7.11), we have, to leading order in Pe_G^{-1},

$$
\epsilon^2 \frac{\partial^2 s_1}{\partial x^2} + \frac{\partial^2 s_1}{\partial y^2} = 0, \qquad (8.32a)
$$

$$
\begin{aligned}
\mathrm{Pe}_G^{-1}\left[\epsilon^2 \frac{\partial}{\partial x}\left(\frac{\partial r_0}{\partial x}\right) + \frac{\partial}{\partial y}\left(\frac{\partial r_0}{\partial y}\right)\right] + \frac{\mathrm{Pe}_G^{-1}}{2}\left[\epsilon^2 \frac{\partial}{\partial x}\left(r_0 \frac{\partial s_1}{\partial x}\right) + \frac{\partial}{\partial y}\left(r_0 \frac{\partial s_1}{\partial y}\right)\right] &= 0 \\
\epsilon^2 \frac{\partial^2 r_0}{\partial x^2} + \frac{\partial^2 r_0}{\partial y^2} + \frac{1}{2}\left[\epsilon^2 \frac{\partial}{\partial x}\left(r_0 \frac{\partial s_1}{\partial x}\right) + \frac{\partial}{\partial y}\left(r_0 \frac{\partial s_1}{\partial y}\right)\right] &= 0. \qquad (8.32b)
\end{aligned}
$$

The boundary conditions at the ends $x = 0$ and $x = -2$ are exactly as given in (7.13) and (7.14) with the appropriate numerical subscript for each function. Similarly, the conditions at the wall are the same as in (7.15). For the boundary conditions at the channel and the GDL, they are exactly the same as in the one-dimensional case, namely (8.13), (8.18), (8.11), and (8.8b):

$$
\begin{aligned}
r_0(x,0) &= 0, \qquad \frac{1}{2}\frac{\partial s_1}{\partial y}(x,0) = -\Phi_{\mathrm{u}} \frac{\partial r_0}{\partial y}(x,0) \\
r_0^{\mathrm{l}}(x,1) &= 1, \qquad s_1^{\mathrm{l}}(x,1) = 0, \quad -2 \le x \le 1.
\end{aligned}
$$

Remark 1. We note that the leading-order equation (8.32b) derived above is slightly simpler than (7.11b). More importantly, we have eliminated Pe_G^{-1} from the equations. Note also that m is also absent from the boundary conditions and the only remaining small parameter is ϵ.

Remark 2. We could further simplify the problem by expanding the solution with respect to ϵ. It is easy to see that the solution will be quasi-1D for $x < 0$ and $x > 0$. However, near $x = 0$, we will have to solve the full 2D problem.

Section 9: Considering the Liquid

Since the transport of liquid water in the porous matrix is of central importance to the problem, we examined this transport problem in isolation without giving consideration to the gas phases, save that gas occupies the space not occupied by liquid water. The resulting system has the advantage of incorporating most of the interesting features of this problem (specifically, thermal and liquid transport). At the same time, the solution is driven by a small number of known and unknown material parameters. Thus, a good calculation of this reduced problem may provide some tools for exploring material parameter regimes and provide valuable inputs, such as the location and amount of liquid water in the matrix, to those studying the interdiffusion of the various gas phases.

At equilibrium, $\tilde{v}$ is uniform. Substituting this fact into (2.8) and solving, the equilibrium vapor content is computed to be

$$\tilde{v}_{\text{eq}} = \frac{\theta_0 \beta_\theta}{\beta_v} \exp\left(-\frac{E_{\text{A}}}{R\tilde{T}_0}\right), \tag{9.1a}$$

where the subscript "eq" stands for "equilibrium" and the subscript 0 pertains to characteristic values. For the numerical calculations, it is more convenient to consider the equilibrium vapor content as a volume fraction. Therefore, we define

$$\Phi_{v,\text{eq}} = \frac{\tilde{v}_{\text{eq}}}{G_{\text{l}}}. \tag{9.1b}$$

To select the parameter value of $\tilde{v}_{\text{eq}}$, we choose $\theta_0 = 10^{-2}$ and $\tilde{T}_0 = 353$ K to model the conditions of the humidified channel above the GDL. The temperature is chosen to represent the channel temperature supplied by Gore (353 K). The vapor content is chosen somewhat arbitrarily to represent the fact the gas in the channel is fully saturated.

Then substituting (9.1b) into (2.7) and (2.9), we obtain

$$\nabla \cdot [D_\theta(\theta) \nabla \theta] - \left[\beta_\theta \theta \exp\left(-\frac{E_{\text{A}}}{R\tilde{T}}\right) - \beta_v G_{\text{l}} \Phi_{v,\text{eq}}\right] = 0, \tag{9.2a}$$

$$\nabla \cdot \left[\tilde{k}(\theta) \nabla \tilde{T}\right] - \rho_\theta L \left[\beta_\theta \theta \exp\left(-\frac{E_{\text{A}}}{R\tilde{T}}\right) - \beta_v G_{\text{l}} \Phi_{v,\text{eq}}\right] = 0, \tag{9.2b}$$

where $\tilde{k}(\theta)$ is given in (2.10).

Having $D_\theta(0) = 0$ as is the case in (2.3b) presents computational difficulties because $\theta = 0$ on portions of the boundaries, necessitating very steep boundary layers there. For this reason, we choose to regularize the problem slightly by introducing a small regularization parameter δ into (2.3b):

$$D_\theta(\theta) = A\left(\delta + 1 - e^{-B\theta}\right)^p. \tag{9.3}$$

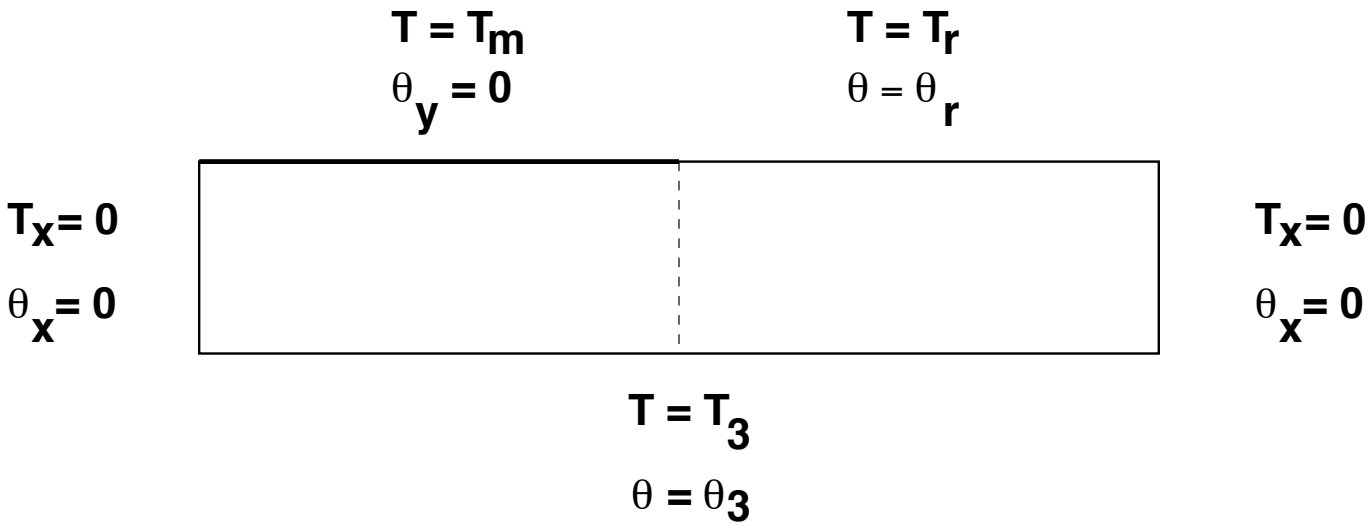

Figure 9.1. Schematic of numerical problem.

Parameter	Value	Parameter	Value
B	5	T_{m} (K)	353
E_{A} (J/kg)	4.07×10^4	T_{r} (K)	353
k_{C} (W m^{-1}K^{-1})	0.3	$\beta_v v_{\mathrm{l}}$ (s^{-1})	4.7
k_θ (W m^{-1}K^{-1})	0.67	β_θ (s^{-1})	3.41×10^4
p	1	$\rho_\theta L$ (J/m^3)	4.07×10^7
T_3 (K)	355	θ_3	0
		θ_{r}	0

Table 9.1. Parameter values for numerical simulations.

If $\delta \gg B\theta$ in the physical domain, we expect and obtain linear behavior. Calculations in the nonlinear regime where $\delta \approx B\theta$ would provide some insight into how the material properties affect liquid water transport in the GDL. Hopefully, asymptotic modeling of the boundary would best inform computations in regimes where $\delta \ll B\theta$, but this is beyond the scope of this workshop.

The geometry of the problem together with the boundary conditions are shown in Figure 9.1; the parameters used are listed in Table 9.1. Values of T and θ were supplied by Gore. The choice of θ_{r} and θ_3 is motivated by (2.16e) and (2.19b). The rationale for this is that there should be no liquid water on the membrane and any liquid water at the channel interface is wicked away. With regard to $D_\theta(\theta)$, we chose the values of B and p for historical reasons.

We used a Chebyshev discretization of the spatial domain. For the steady calculations, we performed Newton iterations to reduce the residuals of (9.2) to a specified tolerance, at which time the approximate system is considered solved.

Our computations focused on the impact of the (unknown) material properties of the GDL and how these would affect moisture transport. It is important to appreciate that the scales used for θ are not relevant in these calculations because the GDL's material properties have not been characterized. The only issue we explore computationally is

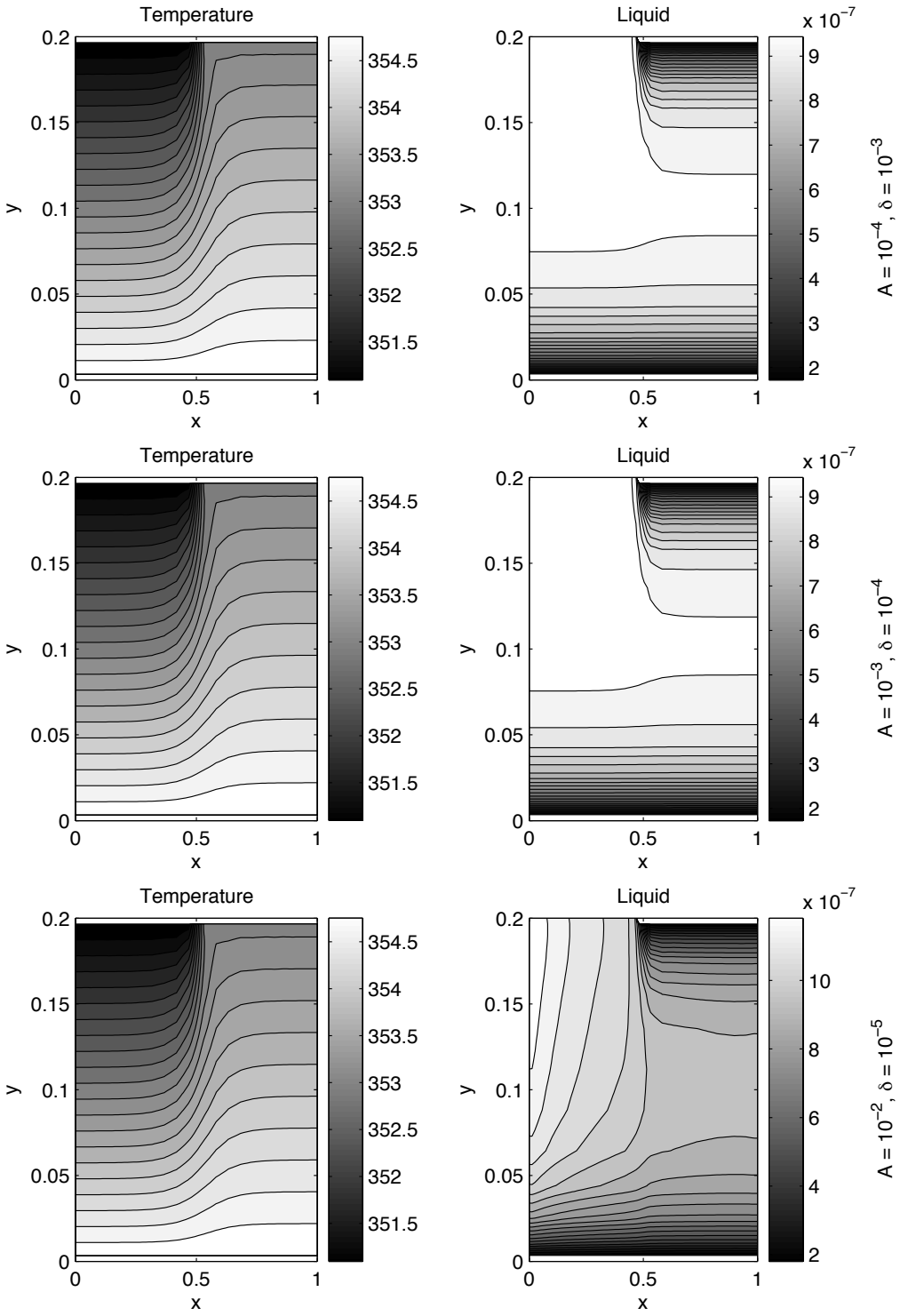

Figure 9.2. Spectral computations of (9.2), the hydrothermal equilibrium in GDL. All quantities used for the calculation are known physical constants or parameters supplied by Gore. The only unknowns are A, p, δ, and B, which characterize our model hydraulic diffusivity. The first figure is essentially linear since variations in θ have little impact on D_θ. As δ decreases, nonlinear behavior becomes more pronounced to a point where the diffusivity varies by a factor of two depending upon the moisture content in the last calculation ($\delta = 10^{-5}$).

regimes where the presence of liquid water effects insignificant or significant change in the liquid diffusivity. Thus, differing magnitudes of θ should be considered relative to the size of D_θ.

For all experiments, we maintained $A\delta$ at a constant value of 10^{-7}. In all cases, we expect the liquid water content to remain small, roughly $\theta \approx 10^{-7}$ at its peak value. The key issue is to explore the impact of nonlinearity on this problem. We found that that the nonlinearity in Richard's equation through D_θ is significant if we consider solutions for $\delta = 10^{-3}$, 10^{-4} and 10^{-5}, as shown in Figure 9.2.

We see that the material nonlinearity can have a substantial impact on the distribution of liquid water throughout the GDL. When water condenses in the linear regime ($\delta = 10^{-3}$), moisture forms in a horizontal band, possibly obstructing the flow of gas to and from the membrane. On the other hand, in the nonlinear parameter regime ($\delta = 10^{-4}, 10^{-5}$), we see that liquid water remains confined under the carbon plating, leaving a clear passage for gas flow. In all calculations, we observed little or no impact on thermal transport.

Section 10: All Phases Together

This section considers the case where both liquid water and water vapor are present together. The model in this section is a simple one—definitely not the last word in describing water in the GDL. Throughout this section, pressure is assumed constant and no convection is allowed. Thus we may reduce our domain to $-2 \le x \le 0$ as in sections 4 and 5.

In addition, (4.1)–(4.3) can be taken as the starting point for the system of equations modeling the interior of the GDL. There are, however, two things that must be changed to handle the presence of liquid water: first a new equation must be added describe the transport of liquid water, and second there must be a source/sink term that describes how water condenses/evaporates. The new equation is basically (2.7), but the source/sink term is somewhat different from what was presented earlier. The source/sink term used here is that used in [13]; condensation/evaporation is proportional to S, where $S > 0$ (oversaturation) implies condensation and $S < 0$ (undersaturation) implies evaporation.

As described above, the equations for the temperature and oxygen concentration do not change, so we use (4.1) and (4.2):

$$\epsilon^2 \frac{\partial^2 T}{\partial x^2} + \frac{\partial^2 T}{\partial y^2} = 0. \tag{10.1}$$

$$\epsilon^2 \frac{\partial^2 u}{\partial x^2} + \frac{\partial^2 u}{\partial y^2} = 0, \tag{10.2}$$

The equations for the water must now be augmented by the condensation/evaporation term as follows:

$$\epsilon^2 \frac{\partial^2 v}{\partial x^2} + \frac{\partial^2 v}{\partial y^2} = \alpha S, \tag{10.3}$$

$$\epsilon^2 \frac{\partial^2 W}{\partial x^2} + \frac{\partial^2 W}{\partial y^2} = -\alpha S \sqrt{\frac{\rho_v}{\rho_\theta}}, \tag{10.4}$$

where $S(v,t)$ is given by (4.40), ρ_v is the density of water vapor and α is the proportionality constant. Further derivation of the form of (10.4) may be found in [13].

The boundary conditions for T, u and v are the same as in Section 5. Since W is simply proportional to θ, we see from section 2 that there are no-flux conditions everywhere except at the inlet channel ($y = 1$, $-2 < x < -1$); at this inlet $W = 0$. These conditions are consistent with only water vapor being created at the CCL/GDL interface, and therefore that liquid water is created only by condensation inside the GDL. Since any net creation of liquid water in the GDL must be balanced by an outward flow somewhere, one would expect there to be at least a small amount of liquid flowing out of the channel.

Since the equations and boundary conditions that describe the temperature and oxygen are unchanged from those in Section 5, the temperature (T) and oxygen (u) profile

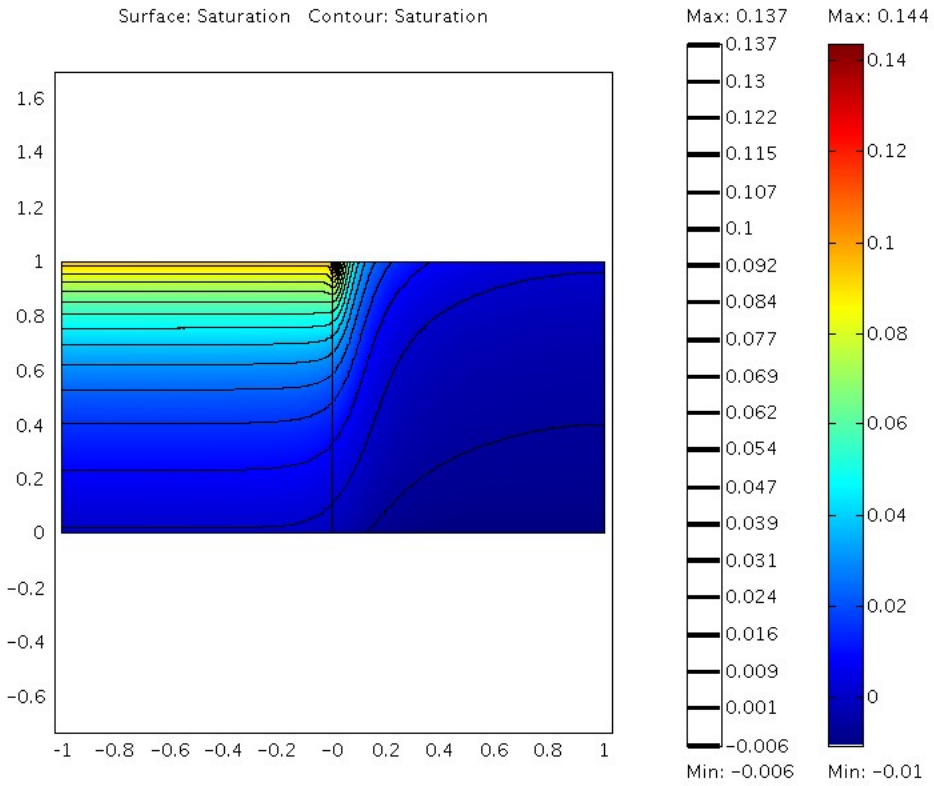

Figure 10.1. Saturation when both liquid water and vapor are present.

in the GDL are also essentially unchanged (they change only because of the presence of u in the boundary conditions at the reaction interface). The possibility of converting water vapor into liquid water causes the saturation to be significantly reduced, and the nature of the profile to change. Indeed in Figure 10.1, one can see that, unlike any of the previous cases, there is now a region in the GDL away from the channel near the CCL where the GDL is under saturated. Also the region of greatest saturation is now just under the channel inlet; this is due to the 100% vapor saturation of the inlet gas. The vapor (v) profile in Fig. 10.2 is also changed since vapor is now flowing into the GDL both from the channel inlet and from the reaction interface, while the conversion of vapor into liquid water in the interior of the GDL leads to a minimum in the vapor profile near $y = 0.5$ for $x < 0$. The liquid water volume pore fraction (W) is in fact very slight; in Fig. 10.3, at a maximum only about 1.65% of the pore space is occupied by liquid water. This level would seem well below what would cause a transport problem for oxygen across the GDL.

Additional mathematical work on this combined liquid/vapor problem is needed to better understand these numerical results. However, we note that since the problems for T and u do not change and essentially can be solved separately, some asymptotic results may be possible.

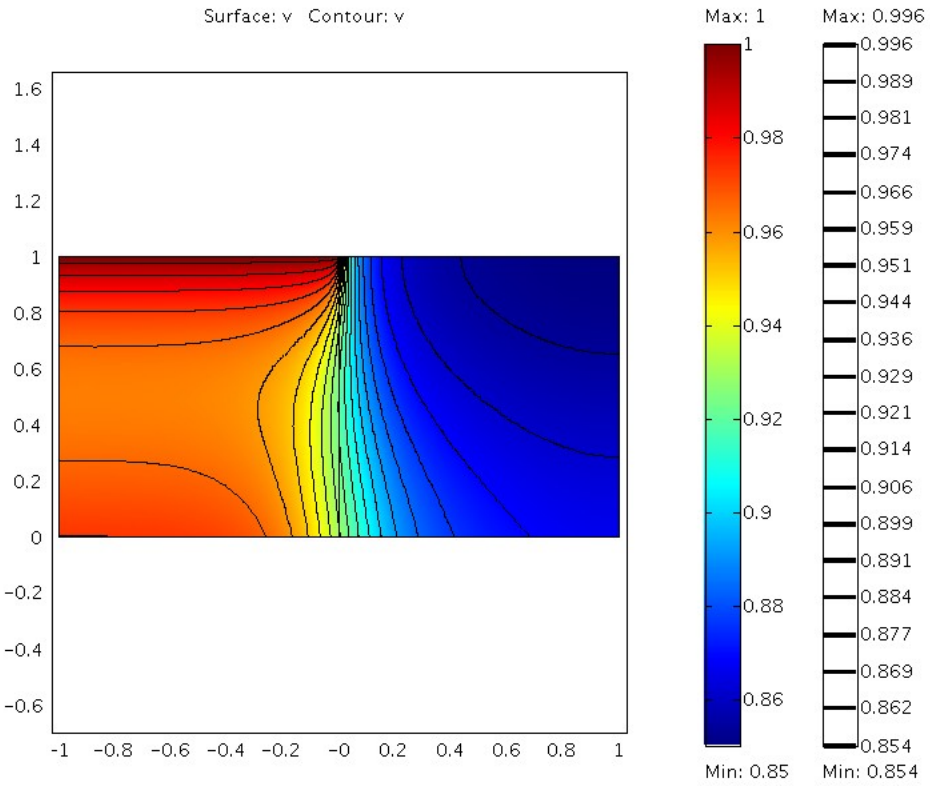

Figure 10.2. Vapor concentration v. Notice the trough near $y = 0.5$, $-1 < x < 0$.

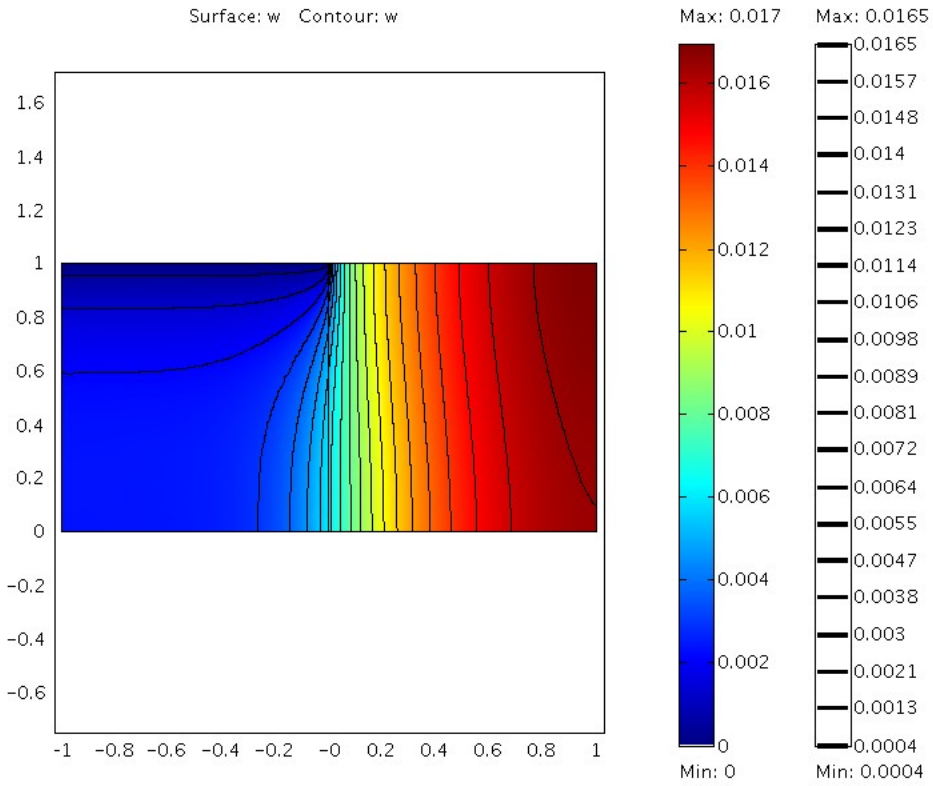

Figure 10.3. Liquid water pore volume fraction W. This fraction is everywhere under 1.7%.

Section 11: Conclusions and Further Research

In this report, we have summarized a variety of findings emerging from different subgroups within our team. First, we have produced a detailed asymptotic picture of gas and heat transport in the dry regime. Second, we have performed some analysis of two-gas phase interdiffusion in the GDL, which allows us to track both gaseous species simultaneously.

Third, we have performed computations of hydrothermal transport to try to understand the role of the material properties on the liquid water and heat transport. Finally, we present calculations of both liquid and vapor phase water in the GDL.

Upon examining the results these different approaches, we offer the following conclusions:

1. The thermal distribution across the GDL is driven entirely by the temperature boundary conditions. No team found any physical process that would substantially alter the heat transfer properties of the GDL. One possible exception would be significant water buildup in the layer, but this is an undesirable regime for other reasons.
2. Liquid water accumulates under the carbon plating first. This comes as no surprise since the carbon plating is impermeable to liquid water, but every avenue of investigation confirms this fact.

We offer the following suggestions and recommendations:

1. From both an analytical and computational perspective, the problem can be reduced by decoupling the heat transfer problem entirely. That is, given complete boundary data, one could solve the heat transfer problem without any consideration of liquid water or gas transport. Then this solution can be used as an input to other processes in the GDL. This simplifies the modeling considerably and is justified by the work contained in this report.
2. The asymptotic solutions determined in this report may be used to inform numerical schemes or analyses in extreme parameter regimes where there would be sharp layers near the boundaries.
3. Our simulations suggest that the material properties of the GDL could have a huge impact on how liquid water is stored in the layer. Thus, it is essential that some experimental understanding of moisture-dependent transport in the GDL be developed.

Directions for future research:

1. The next obvious step would be to improve the liquid/vapor phase water transport model, and take our own advice above to treat heat separately as an input. The vapor equilibrium assumption can easily be relaxed to follow more closely the approach of Philip & De Vries.
2. Since the GDL is a component of a larger fuel cell system, the interdiffusion of gases requires more effort and attention.

Appendix A: Parameter Values

Here are the values of the relevant parameters. First we write down the dimensions of the device:

$$h = 0.02 \text{ cm}, \tag{A.1a}$$
$$d = 0.1 \text{ cm}. \tag{A.1b}$$

Thus we have that

$$\epsilon = \frac{h}{d} = 0.2. \tag{A.2}$$

Next we focus on the temperature. We have

$$T_{\text{m}} = 353 \text{ K}, \tag{A.3a}$$
$$T_{\text{l}} = 355 \text{ K}, \tag{A.3b}$$
$$\tilde{k}_{\text{C}} = 3 \times 10^{-3} \, \frac{\text{W}}{\text{cm} \cdot \text{K}}, \tag{A.4}$$
$$\tilde{q}_T = 0.3 \, \frac{\text{W}}{\text{cm}^2}. \tag{A.5}$$

Substituting (A.1a) and (A.3)–(A.5) into (4.6c), we have

$$q_T = \frac{\tilde{q}_T h}{\tilde{k}_{\text{C}}(T_{\text{l}} - T_{\text{m}})} = \frac{(0.3 \, \text{W/cm}^2)(0.02 \text{ cm})}{(3 \times 10^{-3} \, \text{W/(cm} \cdot \text{K))}(2 \text{ K})} = 1. \tag{A.6}$$

The diffusion coefficients for the gases can be estimated:

$$D_u = 0.2 \, \frac{\text{cm}^2}{\text{s}}, \tag{A.7a}$$
$$D_v = 0.2 \, \frac{\text{cm}^2}{\text{s}}. \tag{A.7b}$$

To calculate u_{l} and v_{l}, we first note that the pressure in the left channel is

$$P_{\text{l}} = 1 \text{ atm} = 1.013 \times 10^6 \, \frac{\text{g}}{\text{cm} \cdot \text{sec}^2}. \tag{A.8}$$

Then using the ideal gas law, we have that G_{l}, the molar density of all the gases together in the left channel, is given by

$$G_{\text{l}} = \frac{P_{\text{l}}}{RT_{\text{l}}} = \frac{1 \, \text{atm}}{(82.05 \text{ cm}^3 \cdot \text{atm/mol/K})(355 \text{ K})} = 3.43 \times 10^{-5} \, \frac{\text{mol}}{\text{cm}^3}. \tag{A.9}$$

Then given that the molar fractions of oxygen and water vapor in the channel are given by

$$\Phi_u = 0.105, \qquad \Phi_v = 0.5,$$

we get the molar densities in the channel that we desire:

$$u_{\mathrm{l}} = \Phi_u G_{\mathrm{l}} = (0.105)\left(3.43 \times 10^{-5}\,\frac{\mathrm{mol}}{\mathrm{cm}^3}\right) = 3.60 \times 10^{-6}\,\frac{\mathrm{mol}}{\mathrm{cm}^3}, \tag{A.10a}$$

$$v_{\mathrm{l}} = \Phi_v G_{\mathrm{l}} = (0.5)\left(3.43 \times 10^{-5}\,\frac{\mathrm{mol}}{\mathrm{cm}^3}\right) = 1.72 \times 10^{-5}\,\frac{\mathrm{mol}}{\mathrm{cm}^3}. \tag{A.10b}$$

We also have values for the fluxes:

$$\tilde{q}_u = 2.6 \times 10^{-6}\,\frac{\mathrm{mol}}{\mathrm{cm}^2 \cdot \mathrm{s}}, \tag{A.11a}$$

$$\tilde{q}_v = 5.2 \times 10^{-6}\,\frac{\mathrm{mol}}{\mathrm{cm}^2 \cdot \mathrm{s}}. \tag{A.11b}$$

Substituting (A.1a), (A.7), (A.10), and (A.11) into (4.6a) and (4.6b), we have values for the dimensionless fluxes:

$$q_u\epsilon^2 = \frac{\tilde{q}_u h}{D_u u_{\mathrm{l}}} = \frac{(2.6 \times 10^{-6}\,\mathrm{mol}/(\mathrm{cm}^2 \cdot \mathrm{s}))(0.02\ \mathrm{cm})}{(0.2\,\mathrm{cm}^2/\mathrm{s})(3.60 \times 10^{-6}\,\mathrm{mol}/\mathrm{cm}^3)} = 7.22 \times 10^{-2}, \tag{A.12a}$$

$$q_u = \frac{7.22 \times 10^{-2}}{(0.2)^2} = 1.81, \tag{A.12b}$$

$$q_v\epsilon^2 = \frac{\tilde{q}_v h}{D_v v_{\mathrm{l}}} = \frac{(5.2 \times 10^{-6}\,\mathrm{mol}/(\mathrm{cm}^2 \cdot \mathrm{s}))(0.02\ \mathrm{cm})}{(0.2\,\mathrm{cm}^2/\mathrm{s})(1.72 \times 10^{-5}\,\mathrm{mol}/\mathrm{cm}^3)} = 3.02 \times 10^{-2}, \tag{A.13a}$$

$$q_v = \frac{3.02 \times 10^{-2}}{(0.2)^2} = 7.55 \times 10^{-1}. \tag{A.13b}$$

For $\tilde{c}_u$, we have the following value:

$$\tilde{c}_u = 0.7\,\frac{\mathrm{cm}}{\mathrm{s}}. \tag{A.14}$$

Therefore, from (5.2) we have

$$c_u = \frac{\tilde{c}_u h}{D_u} = \frac{(0.7\,\mathrm{cm/s})(0.02\ \mathrm{cm})}{0.2\ \mathrm{cm}^2/\mathrm{s}} = 0.07, \tag{A.15}$$

$$c_v\epsilon^2 = \frac{2\tilde{c}_u u_{\mathrm{l}} h}{D_v v_{\mathrm{l}}} = \frac{2(0.7\,\mathrm{cm/s})(0.02\ \mathrm{cm})(3.60 \times 10^{-6}\,\mathrm{mol}/\mathrm{cm}^3)}{(0.2\ \mathrm{cm}^2/\mathrm{s})(1.72 \times 10^{-5}\,\mathrm{mol}/\mathrm{cm}^3)} = 2.93 \times 10^{-2}, \tag{A.16a}$$

$$c_v = \frac{2.93 \times 10^{-2}}{(0.2)^2} = 7.33 \times 10^{-1}. \tag{A.16b}$$

To calculate c_T, we must examine the reaction to see the energy produced. The formula is given by

$$\tilde{c}_T = (\tilde{c}_u)\,(4 \text{ electrons/reaction})\,F\left(\frac{0.6 \text{ V}}{2}\right).$$

Here F is Faraday's constant, 0.6 V is the potential in the device, and we divide by 2 because we assume that half the heat goes back into the GDL, while the other half remains in the CCL. Using our values, we have from (5.2c) that

$$\begin{aligned}
\tilde{c}_T &= \left(0.7\,\frac{\text{cm}}{\text{s}}\right)\left(\frac{9.65 \times 10^4 \text{ C}}{\text{mol}}\right)(1.2 \text{ V}) = 8.11 \times 10^4\,\frac{\text{W} \cdot \text{cm}}{\text{mol}}. \\
c_T &= \frac{\tilde{c}_T u_{\text{l}} h}{\tilde{k}_{\text{C}}(T_{\text{l}} - T_{\text{m}})} = \left(\frac{8.11 \times 10^4\,\text{W} \cdot \text{cm/mol}}{3 \times 10^{-3}\,\text{W/(cm} \cdot \text{K)}}\right)\frac{(0.02 \text{ cm})(3.60 \times 10^{-6} \text{ mol/cm}^3)}{2 \text{ K}} \\
&= 9.73 \times 10^{-1}.
\end{aligned} \tag{A.17}$$

For the convection work, we also need the pressure in the right channel:

$$P_{\text{r}} = 1.012 \times 10^6\,\frac{\text{g}}{\text{cm} \cdot \text{sec}^2}. \tag{A.18}$$

Thus we see from (2.16c) that

$$\gamma\epsilon^2 = \frac{P_{\text{r}} - P_{\text{l}}}{P_{\text{l}}} = \frac{1.013 - 1.012}{1.013} = 9.87 \times 10^{-4} \tag{A.19a}$$

$$\gamma = \frac{9.87 \times 10^{-4}}{(0.2)^2} = 2.47 \times 10^{-2}. \tag{A.19b}$$

We were given that

$$\kappa_{\text{g}} = 10^{-12} \text{ m}^2 = 10^{-8} \text{ cm}^2. \tag{A.20}$$

We may find values for the viscosity in [13]:

$$\mu = 2.24 \times 10^{-5}\,\frac{\text{kg}}{\text{m} \cdot \text{s}} = 2.24 \times 10^{-4}\,\frac{\text{g}}{\text{cm} \cdot \text{s}}, \tag{A.21}$$

so from (3.8b) we have that

$$\begin{aligned}
\text{Pe}_u &= \frac{\kappa_{\text{g}}(P_{\text{l}} - P_{\text{r}})}{2\mu D_u} = \frac{(10^{-8} \text{ cm}^2)[(1.013 - 1.012) \times 10^6 \text{ g/(cm} \cdot \text{s}^2)]}{2[2.24 \times 10^{-4} \text{ g/(cm} \cdot \text{s)}]D_u} \\
&= \frac{2.232 \text{ cm}^2\text{/s}}{0.2 \text{ cm}^2\text{/s}} = 1.12 \times 10^{-1}.
\end{aligned} \tag{A.22}$$

Since $D_u = D_v$, we see that $\text{Pe}_v = \text{Pe}_u$.

To calculate Pe_G, we must first have a typical value for W, which we obtain from [13], where it is denoted as β:

$$W = 0.1. \tag{A.23}$$

Substituting the values from (A.7), (A.8), (A.21), and (A.23) into (7.12), we obtain

$$\begin{aligned}\mathrm{Pe}_G &= \frac{\kappa_{\mathrm{g}}(1-W)^3 RTG_{\mathrm{l}}}{D\mu} = \frac{(10^{-8}\ \mathrm{cm}^2)(0.9)^3 P_{\mathrm{l}}}{[2.24\times 10^{-4}\ \mathrm{g/(cm\cdot s)}](0.2\ \mathrm{cm}^2/\mathrm{s})} \\ &= 1.63\times 10^{-4}\,\frac{\mathrm{cm}\cdot\mathrm{s}^2}{\mathrm{g}}[1.013\times 10^6\ \mathrm{g/(cm\cdot s^2)}] = 1.65\times 10^2. \end{aligned} \tag{A.24}$$

Lastly, using the values calculated above, we may calculate m:

$$m = \frac{c_u \Phi_u}{\mathrm{Pe}_G} = \frac{(0.07)(0.105)}{1.65\times 10^2} = 4.45\times 10^{-5}. \tag{A.25}$$

Nomenclature

Units are listed in terms of length (L), mass (M), moles (N), time (T), or temperature (Θ). If the same letter appears both with and without tildes, the letter with a tilde has dimensions, while the letter without a tilde is dimensionless. The equation number where a particular quantity first appears is listed, if appropriate.

A: arbitrary constant, variously defined.
B: arbitrary constant, variously defined.
$\tilde{c}$: transfer coefficient, units L/T (5.1a).
D: diffusion coefficient, units L^2/T (2.2a).
d: half-width of GDL segment, units L.
E_{A}: activation energy, units ML^2/NT^2 (2.5a).
f: arbitrary function, variously defined.
$\tilde{G}(\tilde{x},\tilde{y})$: total gas molar density in channel, units N/L^3 (7.2).
g: arbitrary function (4.34b).
h: height of channel, units L.
$\tilde{k}$: thermal conductivity, units $ML/T^3\Theta$ (2.9).
L: latent heat for water, units L^2/T^2 (2.9).
m: dimensionless parameter (7.19).
n: normal direction.
$\tilde{P}(\tilde{x},\tilde{y})$: pressure at position $(\tilde{x},\tilde{y})$, units M/LT^2.
p: arbitrary constant, variously defined.
Pe: Péclet number measuring the ratio of convective to diffusive effects (3.8b).
$\tilde{q}$: imposed flux at CCL, units N/L^2T for concentration flux and M/T^3 for heat flux (4.5a).
R: gas constant, units $ML^2/NT^2\Theta$ (2.5a).
$r(x,y)$: fraction of gas that is oxygen (7.6).
$S(v,T)$: saturation measurement for water vapor (4.40).
$s(x,y)$: dimensionless square of the total gas concentration (7.10).
$\tilde{T}(\tilde{x},\tilde{y})$: temperature at position $(\tilde{x},\tilde{y})$, units Θ.
$\tilde{u}(\tilde{x},\tilde{y})$: concentration of oxygen at position $(\tilde{x},\tilde{y})$, units N/L^3.
$\tilde{\mathbf{V}}(\tilde{x},\tilde{y})$: gas velocity at position $(\tilde{x},\tilde{y})$, units L/T (2.1).
$\tilde{v}(\tilde{x},\tilde{y})$: concentration of water vapor at position $(\tilde{x},\tilde{y})$, units N/L^3.
$W(\cdot,\cdot)$: pore volume fraction of water, value θ/ϕ (2.3a).
$\tilde{x}$: distance along channel measured from graphite centerline, units L.
$\tilde{y}$: distance along channel measured from graphite centerline, units L.
$\mathcal{Z}$: the integers.
z: interior-layer variable, value $(x+1)/\epsilon$ (4.10).
α: condensation/evaporation conversion factor for two-phase model (10.3).
β_v: condensation conversion factor, units L^3/NT (2.7).

β_θ: evaporation conversion factor, units T^{-1} (2.7).
γ: proportionality constant for pressures, value $(P_\mathrm{l} - P_\mathrm{r})\epsilon^{-2}/P_\mathrm{l}$ (2.16c).
δ: small regularization parameter (9.3).
ϵ: small aspect ratio, value h/d.
$\theta(\cdot,\cdot)$: liquuid water volume fraction (2.1).
$\kappa(\theta)$: permeability, units L^2 (2.1).
μ: viscosity of the gas, units M/LT (2.11).
ρ: density, units M/L^3 (2.9).
Σ: sources and sinks due to condensation and evaporation (2.2a).
$\Phi(\tilde{x},\tilde{y})$: volume fraction at position $(\tilde{x},\tilde{y})$ (7.6).
ϕ: porosity.
$\Psi(\theta)$: moisture potential, units T^{-1} (2.1).

Other Notation

C: as a subscript, used to indicate graphite (2.10).
eq: as a subscript, used to indicate equilibrium (9.1a).
G: as a subscript, refers to the variable G (7.12).
g: as a subscript, used to indicate the gas (2.4).
i: as a superscript, used to indicate an interior layer (4.10).
l: as a sub- or superscript, used to indicate the region under the left channel (2.8).
m: as a sub- or superscript, used to indicate the region under the graphite (2.13).
$n \in \mathcal{Z}$: as a subscript, used to indicate an expansion in ϵ (4.7), a normalization factor (9.1a), or a series of transformations.
r: as a subscript, refers to the variable r (8.23).
r: as a sub- or superscript, used to indicate the region under the right channel (2.16a).
s: as a subscript, refers to the variable s (8.22).
sat: as a subscript, used to indicate a saturation value (2.16a).
T: as a subscript, used to indicate temperature (4.5c).
u: as a subscript, used to indicate oxygen (2.4).
v: as a subscript, used to indicate water vapor (2.7).
θ: as a subscript, used to indicate liquid water (2.1).

References

[1] M. Bernardi and M. W. Verbrugge, "A Mathematical Model of the Solid-polymer-electrolyte Fuel-cell." *J. Electrochem. Soc.*, **139**, 1992, 2477–2491.

[2] T. F. Fuller and J. Newman, "Water and Thermal Management in Solid-polymer-electrolyte Fuel-cells." *J. Electrochem. Soc.*, **140**, 1993, 1218–1225.

[3] T. E. Springer, T. A. Zawodzinski, and S. Gottesfeld, "Polymer Electrolyte Fuel Cell Model." *J. Electrochem. Soc.*, **138**, 1991, 2334–42.

[4] C. Marr and X. Li, "Composition and Performance Modeling of Catalyst Layer in a Proton Exchange Membrane Fuel Cell." *J. Power Sources*, **77**, 1999, 17–27.

[5] K. Promislow and J. M. Stockie, "Adiabatic Relaxation of Convective-Diffusive Gas Transport in a Porous Fuel Cell Electrode." *SIAM J. Appl. Math.*, **62**, 2002, 180–205.

[6] J. M. Stockie, K. Promislow and B. Wetton, "A Finite Volume Method for Multicomponent Gas Transport in a Porous Fuel Cell Electrode." *Intl. J. Num. Meth. Fluids*, **41**, 2003, 577–599.

[7] S. Dutta, S. Shimpalee and J. W. Van Zee, "Numerical Prediction of Mass-exchange Between Cathode and Anode Channels in a PEM Fuel Cell." *Intl. J. Heat Mass Transfer*, **44**, 2001, 2029–2042.

[8] L. You and H. Liu, "A Two-phase Flow and Transport Model for the Cathode of PEM Fuel Cells." *Intl. J. Heat Mass Transfer*, **45**, 2001, 2277–2287.

[9] J. R. Philip, "Theory of Infiltration," in *Advances in Hydroscience*, Ven Te Chow, ed. Academic Press, 1969, pp. 215–296.

[10] J. R. Philip and D. A. De Vries, "Moisture Movement in Porous Materials under Temperature Gradients." *Trans. Amer. Geophys. Union*, **28**, 1957, 222–232.

[11] P. Broadbridge and I. White, "Time to Incipient Ponding: Comparison of Analytic, Quasi-analytic and Approximate Predictions." *Water Resources Res.*, **23**, 1988, 2302–2310.

[12] J. M. Stewart and P. Broadbridge, "Calculation of Humidity During Evaporation from Soil." *Adv. in Water Resources,* **22**, 1999, 495–505.

[13] K. Promislow, J. Stockie, and B. Wetton, "A Sharp Interface Reduction for Multiphase Transport in a Porous Fuel Cell Electrode." Submitted to *SIAM J. Appl. Math.*